Waves of light at the bottom of the ocean: insights into the luminous systems of three sea pens (Pennatuloidea, Octocorallia, Anthozoa)

Laurent Duchatelet[1,*,$], Gabriela A. Galeazzo[2,$], Constance Coubris[1], Laure Bridoux[3], René Rezsohazy[3], Marcelo R.S. Melo[4], Martin Marek[5,6], Danilo T. Amaral[7], Sam Dupont[8,9], Anderson G. Oliveira[10], Jérôme Delroisse[11,12]

[1] Marine Biology Laboratory, Earth and Life Institute, University of Louvain – UCLouvain, Belgium
[2] Departamento de Oceanografia Física, Química e Geológica, Instituto Oceanográfico, Universidade de São Paulo, São Paulo, Brazil
[3] Animal Molecular and Cellular Biology, Louvain Institute of Biomolecular Science and Technology, University of Louvain – UCLouvain, Belgium
[4] Departamento de Oceanografia Biológica, Instituto Oceanográfico, Universidade de São Paulo, São Paulo, Brazil
[5] Loschmidt Laboratories, Department of Experimental Biology and RECETOX, Masaryk University, 625 00 Brno, Czech Republic
[6] International Clinical Research Center, St. Anne's University Hospital Brno, Pekarska 53, 656 91 Brno, Czech Republic
[7] Centre for Natural and Human Sciences, Federal University of ABC, Santo André, Brazil
[8] Department of Biological & Environmental Sciences, University of Gothenburg, Fiskebäckskil, Sweden
[9] International Atomic Energy Agency, Environment Laboratories, Principality of Monaco, Monaco
[10] Department of Chemistry and Biochemistry, Yeshiva University, 245 Lexington Ave, New York, NY 10016, USA
[11] Biology of Marine Organisms and Biomimetics, Research Institute for Biosciences, University of Mons, Belgium
[12] Cellular and Molecular Immunology, GIGA Institute, University of Liège, Belgium

* Corresponding authors: Duchatelet Laurent, Laurent.duchatelet@uclouvain.be
$ Both authors contributed equally

Abstract

Bioluminescence is the production of visible light by living organisms. It occurs through the oxidation of specific luciferin substrates catalyzed by luciferase enzymes. Auxiliary proteins such as fluorescent proteins and coelenterazine-binding proteins can modify the wavelength of the emitted light or stabilize reactive luciferin molecules, respectively. Additionally, calcium ions are crucial in the luminescence processes across various species. Despite many bioluminescent organisms, only a few systems have been fully studied, notably the *Renilla* genus among anthozoans, which uses a coelenterazine-dependent luciferase, calcium-dependent coelenterazine-binding protein, and green fluorescent protein.

We investigated the bioluminescence of three sea pen species: *Pennatula phosphorea, Funiculina quadrangularis*, and *Anthoptilum murrayi* (Pennatuloidea, Anthozoa). Their light emission spectra reveal peaks at 510 nm, 513 nm, and 485 nm, respectively. We confirmed the coelenterazine-based reaction in all three species. Using transcriptome analyses, we identified luciferases, fluorescent proteins, and coelenterazine-binding transcripts for *P. phosphorea* and *A. murrayi*. Immunodetection confirmed luciferase expression in *P. phosphorea* and *F. quadrangularis*. We also expressed recombinant *A.*

murrayi luciferase, confirming its activity. We underscore the role of calcium ions in bioluminescence, which is possibly associated with the mechanism of coelenterazine binding and substrate release. The study proposes a model for anthozoan bioluminescence, offering new avenues for futur ecological and functional research on these luminous organisms.

Keywords: Bioluminescence, Luciferase, Coelenterazine, Luciferin-binding protein, Calcium, Luminous system, Pennatulidae, Anthoptilidae, Funiculidae

Introduction

Bioluminescence, the production of visible light by a living organism, involves the oxidation of a luciferin substrate catalyzed by a luciferase enzyme. In some bioluminescent system, luciferase and luciferin form a stable complex known as "photoprotein" [1]. Luciferases *sensu lato* (*i.e.,* luciferases *stricto sensu* and photoproteins) are classically considered taxon-specific (*i.e.,* each clade is characterized by its own luciferase) [2]. Nevertheless, analogous or even homologous luciferases can sometimes be used by phylogenetically distant luminous organisms [3]. At least 12 distinct types of luciferases, *sensu lato,* have been recently described [3].

When the photogenic reaction occurs, the generated light is defined by a color that can differ depending on luciferin, but also on the amino acid sequence and structure of the luciferase [4-7]. In some cases, the light emitted by an organism results from an interaction between the luciferase and a fluorescent protein [4]. The fluorescent protein absorbs photons emitted by the bioluminescence reaction and becomes excited. It then re-emits light at longer wavelengths before returning to the ground state. For example, Green Fluorescent Protein (GFP) emits green light after absorbing blue light primarily emitted by the luciferin-luciferase reaction [1,5].

Luminous anthozoans are distributed among four orders: Actiniaria, Zoantharia, Malacalcyonacea (including four luminous families), and Scleralcyonacea (including 18 luminous families mainly spread into the Pennatuloidea superfamily; **Table S1**). The bioluminescence system of *Renilla reniformis* (Pallas, 1766) (Pennatuloidea) has been extensively characterized. It involves the most widespread luciferin in marine environments, the coelenterazine (6-(4-hydroxyphenyl)-2-[(4-hydroxyphenyl)methyl]-8-(phenylmethyl)-7H-imidazo[1,2-a]pyrazin-3-one), and a coelenterazine-dependent luciferase (*R*Luc-type) [9,10,15]. This luciferase is homologous to bacterial haloalkane dehalogenases, which are assumed to have been horizontally transferred during evolution [3]. In addition, more recent descriptions of similar bioluminescent molecular components in different pennatulaceans are sparse [8-16] (**Table S1**). Bessho-Uehara et al. (2020) demonstrated the widespread occurrence of coelenterazine-based *R*Luc-type luciferase across deep-sea pennatulacean species, such as *Distichoptilum gracile* (Verrill, 1882), *Umbellula* sp., *Pennatula* sp., and *Funiculina* sp. [12]. In addition, *R*Luc-type luciferases are also found in phylogenetically distant organisms such as echinoderms (*Amphiura filiformis* (Müller, 1776); [17]) and tunicates (*Pyrosoma atlanticum* (Péron, 1804); [18]). Luminescence-associated

molecules, such as coelenterazine-binding protein (CBP) and GFP have also been identified in sea pansy and other pennatulaceans [15,19-24]. Additionally, the calcium ion cofactor has been demonstrated to be indirectly involved in light production in *R. reniformis* and *Veretillum cynomorium* (Pallas, 1766) [25,26]. CBP depends on calcium ions as cofactors to release luciferin, which allows light production in *R. reniformis* [27].

Light production in sea pens occurs within specific endodermal cells (*i.e.,* photocytes), depending on the species, in the tissues of autozooid and siphonozooid polyps [28-30]. These photocytes often exhibit green autofluorescence [31,32]. To date, bioluminescent pennatulaceans display nervous catecholaminergic control of light emission, with adrenaline- and noradrenaline-triggered waves of flashes [33,34]. Although no experimental behavioral evidence has been obtained, the ecological function of pennatulacean luminescence may serve as an aposematic signal, avoiding predation through misdirection or burglar alarm effects [2,35]. The current data and gaps in the anthozoan bioluminescence data are presented in **Table S1**.

Despite extensive characterization of the *Renilla* bioluminescence system, the molecular mechanisms and components involved in the bioluminescence of other sea pen species remain largely unexplored. This study aimed to explore the unique bioluminescent systems of three sea pen species, the pennatulid *Pennatula phosphorea* (Linnaeus, 1758), funiculinid *Funiculina quadrangularis* (Pallas, 1766), and anthoptilid *Anthoptilum murrayi* (Kölliker, 1880), focusing on their biochemical and molecular aspects. A multidisciplinary study using luminometric assays, transcriptome analyses, phylogenetic analyses, 3D protein modeling, and immunodetection revealed the basis of the bioluminescent system of these soft coral sea pens. Cross-reaction luminometric results highlight the involvement of a *Renilla*-like luciferase in *P. phosphorea* and *F. quadrangularis*, both shallow water species, with coelenterazine as the substrate for all three bioluminescent systems. Besides, *P. phosphorea* and *A. murrayi de novo* transcriptome analyses corroborate (*i*) the homology of both retrieved luciferase sequences with the *Renilla* luciferase, (*ii*) the *in silico* presence of CBPs and a GFP homologous to the one found in other bioluminescent anthozoans. The luciferase expression sites within the autozooids and siphonozooids of *P. phosphorea* and autozooids of *F. quadrangularis* are described. The presence of GFP was also pinpointed in *P. phosphorea* through comparative microscopy. Finally, the involvement of calcium in the light emission process of *P. phosphorea* and *F. quadrangularis* is described.

Materials and methods

Specimen collection

In July 2022 and 2023, common sea pens, *Pennatula phosphorea* (n = 30), were collected in Gullmarsfjord, Sweden, using a small 1 m aperture dredge at 35–40 m depth. Similarly, tall sea pens, *Funiculina quadrangularis* (n = 11), were sampled using the same methodology at a depth of 40 m in July 2023. Animals were brought back to the Kristineberg

Marine Research Station (Fiskebäckskil, Sweden) and maintained under dark conditions in fresh, running, deep-sea water pumped from the adjacent fjord.

Specimens of *Anthoptilum murrayi* (n = 3) were collected during the DEEP-OCEAN expedition off the southeast coast of Brazil aboard R/V Alpha Crucis. The collection was carried out using a demersal trawl net with 19 m in the lower rope, mesh sizes of 100 mm in the body and wings, and 25 mm in the codend at an average depth of 1,500 m. Collection permits were issued by the Instituto Chico Mendes de Conservação da Biodiversidade (SISBIO permits #28054-4, 82624-1), Secretaria da Comissão Interministerial para Recursos do Mar da Marinha do Brasil (Portaria No. 223). After hoisting the net, all collected organisms were sorted, and A. murrayi specimens were promptly frozen in liquid nitrogen. These samples were maintained at the Oceanographic Institute of the University of São Paulo (São Paulo, Brazil) in an -80 ºC ultra-freezer.

Dissection

Specimens of *P. phosphorea* and *F. quadrangularis* were anesthetized by immersion in $MgCl_2$ (3.5%) for 30 minutes [34]. For each tested specimen of *P. phosphorea*, (*i*) the pinnules were dissected and weighed, and (*ii*) the rachis was divided into three equivalent portions and weighed. For specimens of *F. quadrangularis*, the rachis bearing the polyps was split into 3 cm-long segments. Sea pen pinnules and rachises were either directly used for biochemical assays or rinsed for 3 h in fresh running deep-sea water for pharmacological calcium assays. Other specimens were directly fixed in PFA 4% phosphate buffer saline (123 mM NaCl, 2.6 mM KCl, 12.6 mM Na_2HPO_4, 1.7 mM KH_2PO_4, pH 7.4) for further immunodetection techniques.

Owing to the constraints associated with harvesting organisms at depth (*e.g.*, trawling damage), the survival of *A. murrayi* was impossible to maintain. Therefore, all measurements were performed on the frozen samples.

Light emission spectrum of Anthoptilum murrayi

The bioluminescence spectrum of *A. murrayi* was obtained using frozen coral pieces thawed and hydrated with deionized water. The spectra were recorded using a cooled CCD camera (LumiF SpectroCapture AB-1850). Measurements were conducted in triplicate, with an exposure time of 2 min at room temperature.

Luminescent system biochemistry

Eleven specimens of *P. phosphorea* were used for biochemical analysis. Tests were performed for the pinnules (n = 40), rachises (n = 10), and peduncles (n = 10). Pinnule locations along the axis were observed and classified as upper, middle, and lower, depending on the attachment position on the rachis, as in Duchatelet et al., 2023 [34]. Five specimens of *F. quadrangularis* were used immediately after dissection for biochemical assays. Measurements were performed independently of the polyp-bearing rachis location among the colonies (n = 10). Deep-frozen tissues from two A. murrayi specimens were used

for this analysis. For the first two species, the central rigid calcified axis of the rachis was removed before starting experiments.

Light emission measurements were performed in a dark room using an FB12 tube luminometer (Tirtertek-Berthold, Pforzheim, Germany) calibrated with a standard 470 nm light source (Beta light, Saunders Technology, Hayes, UK). Light responses were recorded using FB12-Sirius PC Software (Tirtertek-Berthold). Light emission was characterized as follows: (*i*) maximum light intensity (Lmax), expressed in megaquanta per second (10^9 q s^{-1}), and (*ii*) total amount of light emitted (Ltot) over 3 min, expressed in megaquanta. All data were standardized per unit mass (g).

Luciferase and coelenterazine assays

For the luciferase assay, *P. phosphorea* pinnule and rachis and *F. quadrangularis* rachis were placed in 200 µl of Tris buffer (20 mM Tris, 0.5 mM NaCl; pH 7.4) and crushed with mortar and pestle until a homogenized extract was obtained; 20 and 40 µl of the extract was diluted in 180 and 160 µl Tris buffer, respectively. The diluted *P. phosphorea* and *F. quadrangularis* luciferase solutions were injected into two different tubes filled with 5 µl of a 1/200 stock solution of coelenterazine (Prolume Ltd., Pinetop, AZ, USA) in cold methanol (1OD at 430 nm) diluted in 195 µl of Tris buffer. Two measurements of Lmax were recorded and averaged to calculate the maximal light decay rate corresponding to luciferase activity expressed in 10^9 q s^{-1} g^{-1} [1].

For coelenterazine detection, *P. phosphorea* pinnules, rachises, and *F. quadrangularis* rachises were placed in 200 µl of cold argon-saturated methanol and crushed using a mortar and pestle. Then, 5 µl of the methanolic extract was injected into a tube filled with 195 µl of Tris buffer and placed in a luminometer. Afterward, 200 µl of *Renilla* luciferase solution constituted 4 µl of *Renilla* luciferase (Prolume Ltd., working dilution of 0.2 g l^{-1} in a Tris-HCl buffer 10 mM, NaCl 0.5 M, BSA 1%; pH 7.4) and 196 µl of Tris buffer was injected into the luminometer tube. The Ltot was recorded and used to calculate the amount of coelenterazine contained in a gram of pinnule (ng g^{-1}), assuming that 1 ng of pure coelenterazine coupled with *Renilla* luciferase emits 2.52×10^{11} photons [1].

A. murrayi tissues were processed using a Potter-Elvehjem homogenizer in 2 mL of Tris-HCl buffer (50 mM, pH 8.0). Following homogenization, the mixture was centrifuged at 15,000 × g for 10 min at 4°C and the pellet was discarded. The supernatant was used for the light emission assays. For each assay, the mixture comprised 100 µL of supernatant, 397 µL of Tris-HCl buffer (50 mM, pH 7.4), and 3 µL of coelenterazine (Prolume Ltd., Pinetop, AZ, USA), to achieve a final volume of 500 µL with a final concentration of 6 µM.

Long-term light monitoring of coelenterazine production

The *P. phosphorea* specimens (n = 12) were maintained in tanks filled with circulating artificial seawater (ASW; 400 mM NaCl, 9.6 mM KCl, 52.3 mM $MgCl_2$, 9.9 mM $CaCl_2$, 27.7 mM Na_2SO_4, 20 mM Tris; pH 8.2) at temperatures following natural temperature variations encountered in the native fjord (https://www.weather.mi.gu.se/kristineberg/en/data.shtml)

with a 12-12 hours photoperiod. Sea pens were fed weekly with REEF LIFE Plancto (Aqua Medic, Germany), a food devoted of any coelenterazine trace. After six and 12 months, potassium chloride (KCl) depolarization, coelenterazine content, and luciferase activity assays were performed on eight and four specimens, respectively, with two replicates per specimen. Luciferase and coelenterazine assays were performed as previously described. Total depolarization through KCl application allows for rapid estimation of the luminous ability of specimens. For the KCl experiments, luminescence induction was performed on the pinnule and rachis portions placed in a tube luminometer filled with 500 µL of ASW. Then, the light emission was triggered with the addition of 500 µL of a KCl solution (400 mM KCl, 52.3 mM $MgCl_2$, 9.9 mM $CaCl_2$, 27.7 mM Na_2SO_4, 20 mM Tris; pH 8.2), and Ltot was recorded over 3 minutes. The recorded luciferase activity, luciferin content, and KCl response were compared with wild-caught measurements.

De novo transcriptome analyses

The pinnule, rachis, and peduncle tissues of a single *P. phosphorea* specimen were dissected and directly immersed in a permeabilizing RNAlater-Ice (Life Technologies) solution overnight at -20°C, following the manufacturer's protocol. Subsequently, the samples were stored at -80°C and processed for RNA extraction. Total RNA was extracted using the TRIzol reagent. The quality of the RNA extracts (RIN value, fragment length distribution, and 28S/18S ratio) and their concentrations were assessed using an Agilent 2100 bioanalyzer. The BGI company (Beijing Genomics Institute, Hong Kong) performed cDNA library preparation and sequencing using a procedure similar to that previously described [36-38]. High-throughput sequencing was conducted using the BGISEQ-500 platform to generate 100 bp paired-end reads. To exclude low-quality sequences, the raw reads were filtered by removing (*i*) reads with more than 20% of the qualities of the base lower than 10, (*ii*) reads only containing the adaptor sequence, and (*iii*) reads containing more than 5% of unknown nucleotide "N." Quality control of the reads was performed using FastQC software [39]. For *P. phosphorea,* a reference *de novo* transcriptome assembly was then created from the remaining clean reads obtained from the pinnule, rachis, and peduncle tissues using Trinity software [40] (Trinity-v2.5.1; min_contig_length 150, CPU 8, min_kmer_cov 3, min_glue 3, SS_lib_type RF, bfly_opts'-V 5, edge-thr=0.1, stderr'). TGICL software was then used to reduce transcriptome redundancy by assembling the contigs into a single set of longer, non-redundant, and more complete consensus unigenes [41] (Tgicl-v2.5.1; -l 40 -c 10 -v 25 -O '-repeat_stringency 0.95 -minmatch 35 -minscore 35'). Unigenes, defined as non-redundant assembled sequences obtained from assembly and/or clustering [42], can form clusters in which the similarity among overlapping sequences is greater than 70% or singletons that are unique unigenes. For all transcriptomes, unigene expression was evaluated using the "Fragments per kilobase of the transcript, per million fragments sequenced" (FPKM) method [36-37,42]. To obtain annotation for transcriptomes, unigenes were aligned to NCBI Nucleotide (NT), NCBI protein (NR), EuKariotic Orthologous groups (KOG), Kyoto Encyclopedia of Genes and Genomes (KEGG), and UniProtKB/Swiss-Prot databases using

Blastn, Blastx [43], and Diamond [44]. Blast2GO [45] with NR annotation results was used to obtain Gene Ontology annotations according to molecular function, biological process, and cellular component ontologies. InterPro [46] was also used to annotate unigenes based on functional analyses of protein sequences, clustering them into families and predicting the presence of domains or essential amino acid residues. The candidate coding area among the unigenes was assessed using Transdecoder (https://transdecoder.github.io).

A similar procedure was used for the specimen of *A. murrayi*. Whole sea pen tissues (pinnule and peduncle) were dissected, frozen in liquid nitrogen, and stored at -80°C. The total RNA from the sea pen was extracted using the RNeasy Plant Mini Kit (QIAGEN), following the extraction steps according to the manufacturer's instructions. The RNA samples were eluted in DEPC-treated water in two 16 µL steps. RNA samples were treated with DNase I (Invitrogen) to remove potential genomic DNA contamination. Subsequently, to remove impurities and residual DNase I reaction remnants, they underwent a column cleanup process, following the instructions of the RNeasy Plant Mini Kit (QIAGEN). The concentrations of RNA samples were estimated by fluorescence using a Qubit fluorometer (Thermo Fisher Scientific). The integrity of the RNA samples was confirmed by agarose gel electrophoresis (1%) stained with SYBR Safe (Invitrogen), and the RNA was dried at 30°C for 1 h in speed vac mode V-AQ.

The quality of RNA extracts (RIN value, fragment length distribution, and 28S/18S ratio) and their concentration were assessed by RNA concentrations were assessed using an Agilent 2100 bioanalyzer. After QC, mRNA was enriched using oligo(dT) beads. First, mRNA was randomly fragmented by adding a fragmentation buffer. Then, the cDNA was synthesized using an mRNA template and random hexamer primer, after which a custom second-strand synthesis buffer (Illumina), dNTPs, RNase H, and DNA polymerase I were added to initiate second-strand synthesis. After a series of terminal repairs, A ligation, and sequencing adaptor ligation, the double-stranded cDNA library was completed through size selection and PCR enrichment. The GenOne Biotechnologies company (Brazil) performed cDNA library preparation and sequencing (150 bp paired-end reads). To exclude low-quality sequences, the raw reads were filtered by removing (*i*) reads with more than 50% of the qualities of the base lower than 5, (*ii*) reads only containing the adaptor sequence, and (*iii*) reads containing more than 10% of unknown nucleotide "N."

Light emission process-related protein sequence analyses

Potential transcripts of interest were chosen using NCBI online tools according to potential phylogenetic homologies to identify genes involved in the light production process, such as luciferases, green fluorescent proteins, and coelenterazine-binding proteins. These "light emission process-related genes" were searched within the newly generated *P. phosphorea* transcriptome using tBLASTn analysis (1 hit, E-value < $1e^{-20}$). All retrieved unigenes were individually reciprocally searched in the NCBI NR database (Reciprocal BLASTx; 1hit, E-value < $1e^{-20}$). BLAST hits with significant E-values strongly support homologous proteins. *In silico* translation (ExPASy translate tool,

http://expasy.org/tools/dna.html) was performed on the sequences retrieved from the *P. phosphorea* and *A. murrayi* transcriptomes for all putative candidates. Multiple alignments were performed for each predicted protein with their respective homologous "light emission process-related protein" retrieved from the NCBI online tool in other species using Geneious software [47]. Sequence alignments have enabled the identification of luciferase characteristic features, such as catalytic triads [48].

To validate the *P. phosphorea* luciferase retrieved sequence, primers were designed based on *Renilla muelleri* luciferase mRNA (AY015988.1) to amplify the hypothetical luciferase sequence using Primer Blast software (**Table S2**). *P. phosphorea* pinnules were collected and lysed in 300 µL of 50 mM NaOH for 30 min at 95°C with agitation at 800 rpm. The pH was adjusted by adding 60 µL 500 mM Tris-HCl at pH 8. For PCR amplification, the reaction mix contained 1U of Expand Long Template (Roche) with the provided buffer, 400 µM dNTP (#R0191, Life Technologies), and 250 nM of each primer. Amplification was performed as follows: 95°C for 5 min; 35 cycles of denaturation at 95°C for 30 s, hybridization from 52 °C to 55°C for 15 s, and elongation at 68°C for 45–80 s. The final cycle was completed with a final elongation step at 68°C for 7 min. Primer pairs F1-R1, F2-R2, and F8-R2 resulted in amplifications visualized through electrophoresis and ethidium bromide incorporation. Genomic DNA was purified using the Qiagen PCR Purification Kit according to the manufacturer's instructions and sequenced by Microsynth.

Phylogenetic analyses

The predicted sequences of the luciferases (LUC), GFP, and CBPs of *P. phosphorea* and *A. murrayi* were placed into an anthozoan-focused phylogenetic context using maximum likelihood phylogenetic reconstruction [49]. *Renilla*-type luciferase sequences from selected metazoans were collected from public databases based on literature [12,16,17]. GFP sequences from cnidarians were collected from public databases using reference literature [50-53]. CBP sequences from anthozoans were collected from public databases based on literature [54]. Multiple alignments of all sequences were performed using the MAFFT algorithm implemented in the Geneious software and trimmed using TrimAL software [55]. Maximum likelihood phylogenetic analyses were performed using IQ-tree software [56]. Before the analyses, ModelTest [57] was used to select the best-fit evolution model. Trees were edited using the iTOL web tool.

Structural modeling

AlphaFold models of *P. phosphorea* and *A. murrayi* LUC, GFP, and CBP proteins were obtained from the AlphaFold web server (https://alphafoldserver.com/). The structural models were visualized using PyMOL 2.6 (https://pymol.org/). Structural pairwise alignments and calculations were performed using the Dali server (http://ekhidna2.biocenter.helsinki.fi/dali/).

Luciferase and green fluorescent protein immunodetection

Commercial antibodies against *Renilla* luciferase (GTX125851, Genetex) were used to confirm the presence of a *Renilla*-like luciferase. Proteins were extracted from frozen pinnules, rachis, and peduncle samples. Each sample was homogenized on ice in 1000 µl of 2% Triton X-100 in phosphate buffer saline (PBS: 10 mM Tris, pH 7,5; 1 mM EDTA, pH 8,0; 100 mM NaCl) supplemented with protease inhibitors (complete–Mini tablets, Roche). The extract was sonicated and centrifuged at 800 g for 15 min. The supernatant was then collected. The protein concentration in each extract was measured using a PierceTM BCA Protein Assay Kit (Thermo Scientific). Laemmli buffer (Bio-Rad) and β-mercaptoethanol (βMSH, Bio-Rad) were added to each protein extract and the proteins were electrophoretically separated at 200 V for 35 min on 12% SDS-PAGE gels. The separated proteins were electroblotted onto nitrocellulose membranes. The membrane was incubated overnight with the primary anti-*Renilla* luciferase antibody and the secondary antibody (ECL HRP-conjugated anti-rabbit antibody, Life Sciences, NA934VS, lot number 4837492) for 1 h. Antibody detection was performed using the reagents of the detection kit (HRP Perkin-Elmer, NEL 104) following the manufacturer's instructions. The dilution for the primary antibody was 1:2000.

The same primary antibody was used to immunolocalize luciferases within the *P. phosphorea* pinnules, rachis, peduncle tissues, and *F. quadrangularis* polyp tissue. For *whole-mount* immunofluorescence, the dissected samples were blocked with PBS containing 2% Triton X-100 and 6% BSA (Amresco). Samples were then incubated for 48 h with either the anti-*Renilla* luciferase antibody diluted 1:200 in PBS containing 1% Triton X-100, 0.01% NaN_3, and 6% BSA. Visualization of the luciferase signal was performed after 24 h of incubation of the samples at RT in the dark with a fluorescent dye-labeled secondary antibody (Goat Anti-Rabbit, Alexa Fluor 594, Life Technologies Limited) diluted 1:500 in PBS containing 1% Triton X-100, 0.01% NaN_3, and 6% BSA. Samples were mounted (Mowiol 4–88, Sigma) and examined using an epifluorescence microscope (Axio Observer, Zeiss, Oberkochen, Germany) equipped with Zen microscopy software (Zeiss, Oberkochen, Germany). Control sections were incubated in PBS containing 1% Triton X-100, 0.01% NaN_3, and 6% bovine serum albumin (BSA) with no primary antibodies.

Calcium assays

Following the identification of the key proteins involved in the luminescence system, we assessed the role of calcium, another crucial element in the bioluminescence mechanism. Different pharmacological tests were used to investigate the role of calcium in the light-emission process of *P. phosphorea* and *F. quadrangularis* (n = 6 for each species). First, the calcium concentration was tested using three artificial seawater (ASW) solutions with different calcium concentrations (0, 10, and 20 mM $CaCl_2$). To remove any traces of Ca^{2+} ions in the 0 mM $CaCl_2$ -ASW solution, calcium chelators EGTA (4100, Merck) and BAPTA (14513, Merck) were added to the solution at 10^{-5} M final concentrations. Secondly, the effect of a calcium ionophore (A23187; C7522, Merck) was tested to highlight the potential involvement of calcium storage in the light emission process. Third, the involvement of

calcium was tested in the presence of a previously determined triggering agent of light emission in sea pens, adrenaline at 10^{-5} M. Finally, calcium involvement was tested on the effect of the potassium chloride depolarization solution usually employed to trigger the maximum light production in a bioluminescent species.

After rinsing for 3 h, the pinnules of *P. phosphorea* and polyp-bearing rachises of *F. quadrangularis* were placed in luminometer tubes and subjected to various treatments (**Table S3**). Before the experiments, each sample was pre-incubated for 15 min in ASW devoid of calcium (0 mM $CaCl_2$). Data were recorded for 15 minutes using an FB12 tube luminometer (Tirtertek-Berthold, Pforzheim, Germany). Light emission was defined as the total amount of light emitted (L_{tot}) over 15 min, and was expressed in megaquanta. All data were standardized per unit mass (g).

Statistical analysis

All statistical analyses were performed with R Studio (version 2023.03.1 + 446, 2022, Posit Software, USA). Variance normality and equality were tested using the Shapiro–Wilk test and Levene's test, respectively. When these parametric assumptions were met, Student's t-test and ANOVA coupled with Tukey's test were used to perform single or multiple comparisons between groups. When log transformation did not provide normality and homoscedasticity, the nonparametric Wilcoxon test and Kruskal–Wallis test coupled with the Wilcoxon rank-sum test were used to assess whether significant differences were present between the two groups or multiple groups. Differences were considered significant at a minimum *p-value* of < 0.05. Values are graphically illustrated as the mean and standard error of the mean (s.e.m).

Results

Pennatula phosphorea, Funiculina quadrangularis, *and* Anthoptilum murrayi *emit light using a coelenterazine-dependent luciferase.*

Biochemical assays performed on *P. phosphorea*, *F. quadrangularis*, and *A. murrayi* (**Figures 1A-F**) demonstrated a similar response pattern. The cross-reactivity of the extracts with the commercial *Renilla* luciferase highlights the involvement of coelenterazine in the bioluminescent systems of *P. phosphorea*, *F. quadrangularis*, and *A. murrayi* (**Figure 1**). For *P. phosphorea*, the measured amounts of coelenterazine present no statistical differences between the pinnule areas (ANOVA, *p-value* lower-middle = 0.8122; *p-value* lower-upper = 0.9054; *p-value* upper-middle = 0.7014) (**Figure S1**). Similarly, no significant differences were observed between the rachis portions (ANOVA, *p-value* lower-middle = 0.5905; *p-value* lower-upper = 0.8274; *p-value* upper-middle = 0.4634) (**Figure S1**). The mean coelenterazine content per pinnule and rachis were 131.15 ± 29.06 and 70.00 ± 16.79 ng g^{-1}, respectively. Peduncle presents an almost negligible mean value of 0.21 ± 0.01 ng g^{-1}. Comparatively, the

mean coelenterazine content of *F. quadrangularis* polyp-bearing rachis was 3.79 ± 1.20 ng g^{-1}.

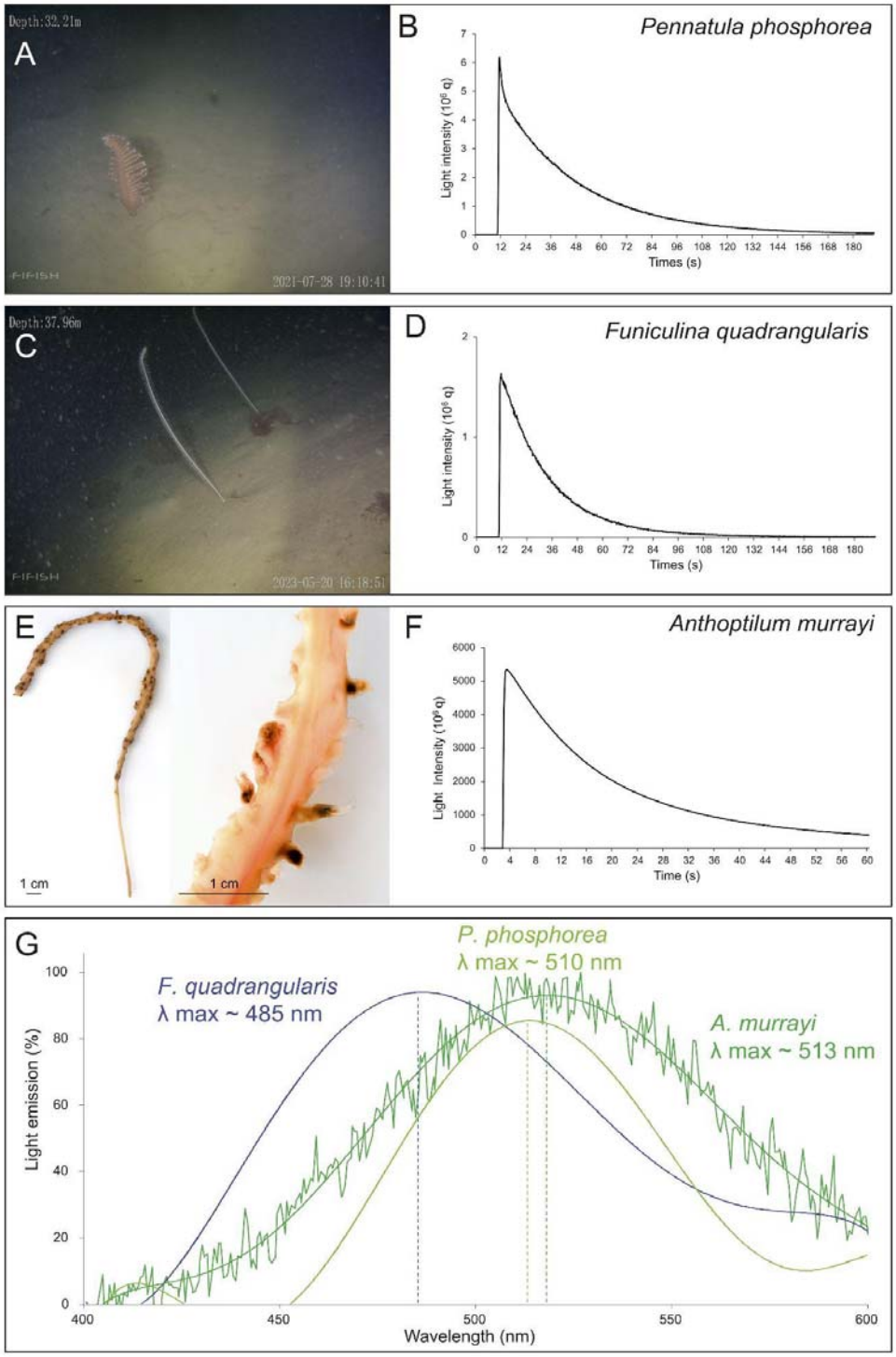

Figure 1. Biochemistry assays. (A) *In situ* images of *Pennatula phosphorea* and (B) typical coelenterazine assay curve for the pinnules. (C) *In situ* images of *Funiculina quadrangularis* and (D) typical coelenterazine assay curve for the 3 cm-long polyp-bearing rachis. (E) Images of *Anthoptilum murrayi* with a zoom on the polyp on the rachis and (F) typical coelenterazine assay curve for the

whole specimen. (G) *Anthoptilum murrayi in vivo* luminescence spectrum compared with the retrieved spectrum of two other species (*P. phosphorea* [58] and *F. quadrangularis* [12]). Pictures (A and C) were provided by Fredrik Gröndahl.

In parallel, a typical coelenterazine assay curve was observed for all three species (**Figures 1B, D, and F)**. Cross-reaction assays using synthetic coelenterazine to measure potential luciferase activity confirmed the involvement of a coelenterazine-based luciferase system in *P. phosphorea* and *F. quadrangularis*. For *P. phosphorea*, luciferase activities in the pinnules show no statistically significant differences across the pinnule areas (ANOVA, *p-value* lower-middle = 0.4963; *p-value* lower-upper = 0.2742; *p-value* upper-middle = 0.6251), with a mean Lmax value of 129.5 ± 22.1 10^9 q g^{-1} s^{-1} (**Figure S1**). Similarly, no statistically significant differences were observed in the Lmax values recorded between rachis portions (ANOVA, *p-value* lower-middle = 0.6360; *p-value* lower-upper = 0.4438; *p-value* upper-middle = 0.2548), with a mean Lmax value of 87.9 ± 16.9 10^9 q g^{-1} s^{-1} (**Figure S1**). Finally, the peduncles tested exhibited a significantly lower mean Lmax value (0.6 ± 0.4 10^9 q g^{-1} s^{-1}) compared to the rachis (ANOVA, *p-value* = 0.0298). Comparatively, *F. quadrangularis* luciferase activity presents a mean Lmax value of 313.8 ± 99.2 10^9 q g^{-1} s^{-1}. To complete the data on the sea-pen light emission spectrum, the *in vivo* light emission spectrum of *A. murrayi* was measured and revealed a peak wavelength at 513 nm (**Figure 1G**).

Pennatula phosphorea *maintains its bioluminescence ability after one year in captivity without an exogenous supply of coelenterazine.*

Prior to the experiment, visual assessments of *P. phosphorea* luminescence were performed in the dark. These observations confirmed that the species maintained the ability to produce visible light even after six–12 months of captivity without any external sources of coelenterazine-containing food.

Measurements of luminescence parameters showed a general decrease in all three parameters for both the pinnules and the rachis (**Figure S2)**. For the pinnules, the maximum light emission shows statistically significant differences upon KCl application (Kruskal-Wallis test, *p-value* = 1.8 10^{-5}), with a mean Ltot value of 361.7 ± 34.6 10^9 q g^{-1} s^{-1} after field collection. This value is statistically different from the mean value observed after six months of captivity (Wilcoxon sum-rank test, *p-value* = 1.5 10^{-6}) but not from the value after 12 months (Wilcoxon sum-rank test, *p-value* = 0.16). The mean Ltot values after 6 and 12 months are 80.5 ± 21.8 and 223.8 ± 84.4 10^9 q g^{-1} s^{-1}, respectively. Coelenterazine content also presented statistically significant differences (Kruskal-Wallis test, *p-value* = 1.3 10^{-5}). The mean coelenterazine content is already drastically reduced after 6 months (30.7 ± 4.5 ng g^{-1}) but remains stable for one year (28.1 ± 4.4 ng g^{-1}) (Wilcoxon sum-rank test, T0 *VS* T6: *p-value* = 0.0001; T0 *VS* T12: *p-value* = 0.0004), without statistical differences between the former two (Wilcoxon sum-rank test, *p-value* = 0.91) (**Figure S2**). Similarly, the luciferase activities decreased over the year and presented statistically significant differences (Kruskal-Wallis test, *p-value* = 0.01). Differences occur between the initial Lmax value (113.2 ± 12.7 10^9 q g^{-1}

462 s^{-1}) and the mean Lmax values of 77.0 ± 16.2 and 43.0 ± 3.7 10^9 q g^{-1} s^{-1} after 6 and 12
463 months, respectively (Wilcoxon sum-rank test, T0 *VS* T6: *p-value* = 0.383; T0 *VS* T12: *p-value*
464 = 0.013; T6 *VS* T12: *p-value* = 0.383) (**Figure S2**). Similar observations occurred for the three
465 parameters recorded on the rachis portions of *P. phosphorea* (**Figure S2**).
466
467 ***De novo transcriptomes of* Pennatula phosphorea *and* Anthoptilum murrayi**
468
469 For *P. phosphorea*, a total of 47.27 million raw reads of 200 bp length were
470 generated from the pinnule library, 47.27 million from the rachis library, and 41.96 million
471 from the peduncle library. Data quality was assessed using FastQC software. Raw reads are
472 available on the NCBI SRA database: *A. murrayi* (PRJNA1144931), *P. phosphorea*
473 (PRJNA1152785). After low-quality reads filtering, the remaining high-quality reads (*i.e.,*
474 45.29 for the pinnule transcriptome, 45,53 for the rachis transcriptome, and 40.29 for the
475 peduncle transcriptome) were used to assemble a reference transcriptome using the Trinity
476 software. The obtained Trinity-predicted transcripts were clustered using TGICL to obtain
477 the final unigenes.
478 In total, 49,510 unigenes (i.e., non-redundant unique sequences) were obtained with
479 a total length of 72,928,901 bp. The average mean length was 1473 bp and the N50 was
480 2350 bp. Among the transcriptome data, 35,439 unigenes for the pinnule dataset, 33,778
481 unigenes for the rachis dataset, and 31,001 unigenes for the peduncle dataset were
482 obtained, with a total of 49,510 different unigenes. The length distributions of the unigenes
483 are shown in **Figure 2A** and the numerical data are summarized in **Tables S4** and **S5**.
484 Of the 46,258 predicted unigenes, 1,690 were found only in the pinnule
485 transcriptome, 1,114 only in the rachis transcriptome, 1, 035 in the peduncle transcriptome,
486 and 36, 934 in the peduncle transcriptome. For descriptive purposes, comparative gene
487 expression analysis was performed by mapping FPKM values (*e.g.,* $\log_{10}$(FPKM value pinnule
488 transcriptome) against $\log_{10}$ (FPKM value rachis transcriptome)) calculated for all predicted
489 unigenes (**Table S6**). However, it has to be clarified that transcriptome data have been
490 generated for new gene discovery, not differential expression analyses, as no biological or
491 technical replication was performed as a part of the study. The main species represented
492 within the unigene annotation of the reference transcriptome was the anthozoan
493 *Dendronephthya gigantea* (Verrill, 1864) (79%) (**Figure 2B**). Of the 49,510 *P. phosphorea*
494 unigenes present in the filtered reference transcriptome, 34,984 showed significant matches
495 with the molecular databases: 33,896 to NR (68.5%, E-value > $1e^{-5}$), 8,818 to NT (17.8%),
496 26,473 to SwissProt (53.5%), 28,290 to KEGG (57.1%), 24,642 to KOG (49.8%), 26,790 to
497 InterPro (54.1%), and 13,742 to GO (27.8%) (**Figure 2C**).
498 For *A. murrayi*, 66,425 unigenes were obtained, with a total length of 54,366,500 bp.
499 The average mean length was 818 bp and the N50 was 1140 bp. The length distributions of
500 the unigenes are shown in **Figure 2D** and the numerical data are summarized in **Tables S4**
501 and **S5**. For descriptive purposes, gene expression analysis was performed by mapping the
502 FPKM values (e.g., $\log_{10}$(FPKM value) calculated for all predicted unigenes (**Table S6**). The

main represented species within the unigene annotation of the reference transcriptome was the anthozoan *Paramuricea clavata* (29%) (**Figure 2E**). Among the 66,425 *A. murrayi* unigenes present in the filtered reference transcriptome, 58,345 were significantly matched to the molecular databases: 41,512 to NR (71.15%, E-value > 1e-10), 11,345 to NT (19.44%), 25,769 to SwissProt (44.16%), 23,549 to KEGG (40.36%), 15,178 to KOG (26.01%), 22,134 to InterPro (37.93%), and 15,178 to GO (26.01%) (**Figure 2F**).

Because of the lack of a reference genome in *P. phosphorea* and *A. murrayi*, and possibly the relatively short length of some unigene sequences, 29.4% and 71,6%, respectively, of the assembled sequences could not be matched to any known genes.

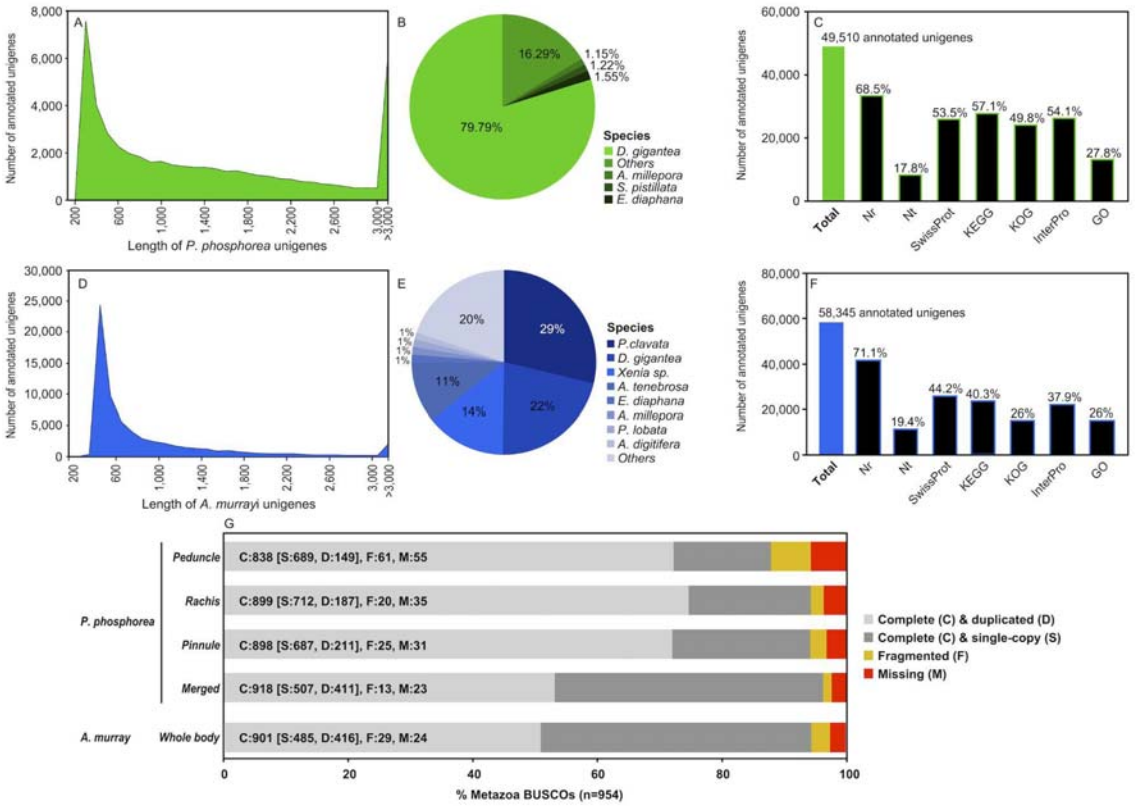

Figure 2. General description of the transcriptomic data. (A) The length distribution of *P. phosphorea* unigenes. (B) Taxonomic annotation of *the P. phosphorea* transcriptome. (C) Global annotation of *P. phosphorea* transcriptome. (D) Length distribution of *the A. murrayi* unigenes. (E) Taxonomic annotation of *A. murrayi* transcriptome. (F) Global annotation of *the A. murrayi* transcriptome. (G) Busco analysis.

Based on Benchmarking Universal Single-Copy Orthologs (BUSCO) analysis, 96.23% of metazoa BUSCO genes were predicted to be complete in the merged *P. phosphorea* transcriptome. In parallel, 1.36% of BUSCO genes were fragmented and 2.41% were missing (**Figure 2G**). Similar results were obtained for *A. murrayi*, with 94.44% complete BUSCO genes found, while 3.04% of BUSCO genes were fragmented, and 2.52% were missing (**Figure 2G**).

525 Analyses of unigene expression revealed a similar proportion of FPKM values in the
526 three tissues (**Figure 3A, B**). Comparatively, a large number of unigenes appeared to be
527 more highly expressed in the pinnule and rachis than in the peduncle tissue (**Figure 3C**). The
528 pinnule and rachis tissues appeared to be more similar in terms of the unigene expression
529 profile. The "Molecular function" GO functional annotations for the 40 most expressed
530 unigenes of each sample of *P. phosphorea* (**Figure 3D**) and the whole animal sample for *A.*
531 *murrayi* (**Figure 3F**) show a classical high expression of molecular actors involved in the
532 cellular machinery and gene regulation. The GO functional annotations for the 40 unigenes
533 with the most pronounced expression differences between tissues, including those highly
534 expressed in one tissue relative to the other and those with lower expression levels, are
535 shown in **Figure 3F**. We did not perform formal differential gene expression analysis, as no
536 replication was performed. Calcium ion binding function (GO: 0005509) appeared to be
537 predominantly expressed in pinnule and rachis tissues, compared to the peduncle (**Figure**
538 **3F**). Similarly, the pinnule tissue (containing the feeding polyp) presented a higher
539 proportion of genes annotated as digestive enzymes (**Figure 3F**).
540

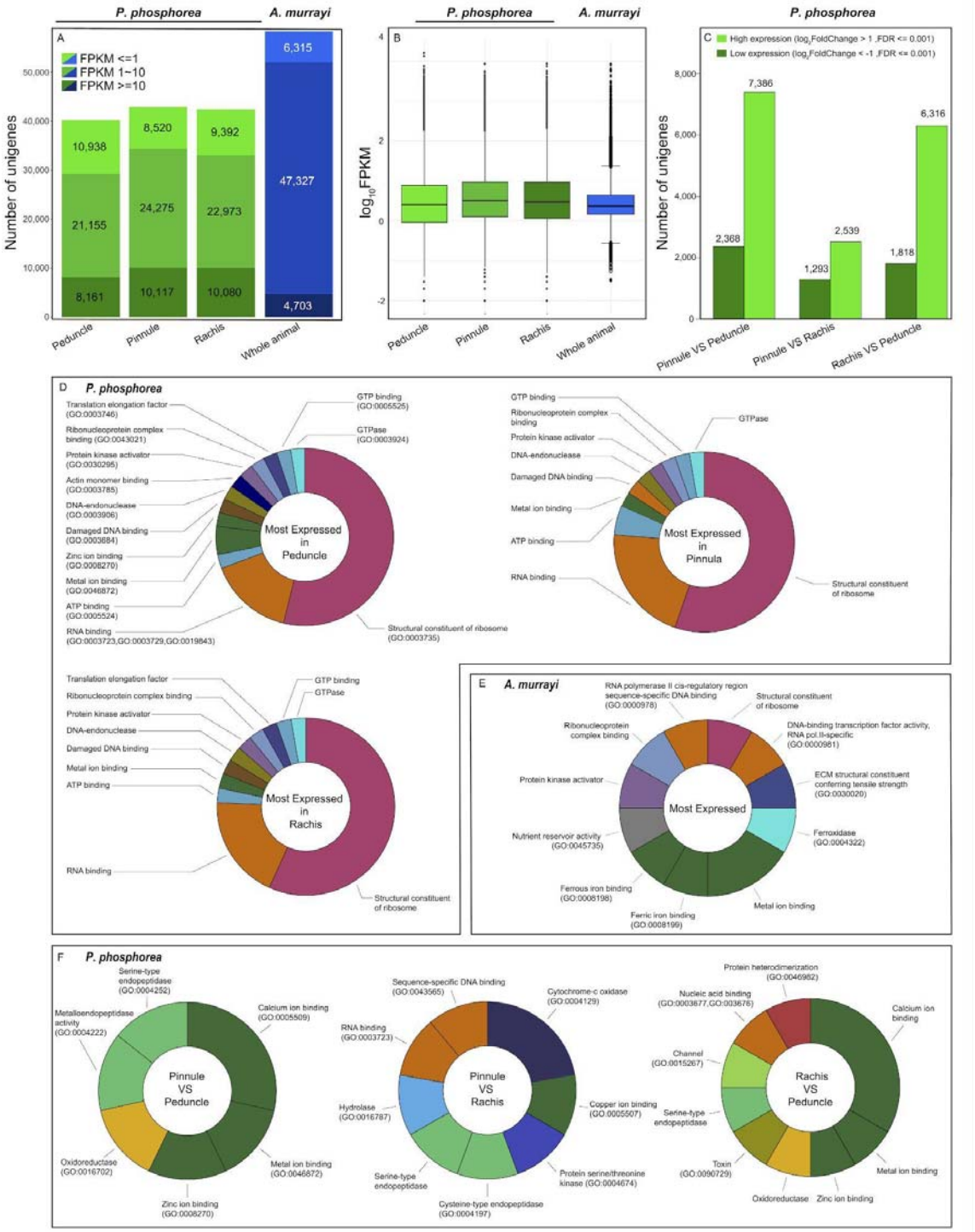

Figure 3. Global gene expression and gene ontology of *Pennatula phosphorea* and *Anthoptilum murrayi* transcriptomic data. (A) Distribution of FPKM expression values across *the P. phosphorea* and *A. murrayi* transcriptomes. (B) Gene expression distribution for each sample. (C) Proportions of unigenes with relatively high or low expression levels in *P. phosphorea* samples. Gene ontology distribution of the 40 most highly expressed unigenes for each sample of *P. phosphorea* (D) and *A. murrayi* (E). (F) Comparison of gene ontology repartition of the 40 most highly expressed unigenes in *P. phosphorea* samples.

Expression of bioluminescence-related genes in Pennatula phosphorea *and* Anthoptilum murrayi

The *P. phosphorea* and *A. murrayi* transcriptomes contained sequences of several predicted luciferases, GFPs, and luciferin-binding proteins. The FPKM values retrieved from each transcriptome are shown in **Table S6**. Reciprocal BLAST analyses revealed that the sequences matched the luciferases, CBPs, and GFPs of Anthozoans.

Several *R*Luc-like enzymes were recovered from both investigated species (*A. murrayi* and *P. phosphorea*). In addition, sequence mining allowed us to recover additional *R*Luc-like sequences from the genomes of *Renilla muelleri* and *R. reniformis*. Phylogenetic analyses revealed three clades of *R*Luc-like enzymes in Pennatulacea (**Figure 4A**). Clade A contains well-known luciferases from *R. muelleri* and *R. reniformis* and probable luciferase sequences from *A. murrayi*, *P. phosphorea,* and *Cavernularia obesa* (Valenciennes, 1850). Interestingly, clade A did not contain any sequences from the non-luminous species. Clade B, in comparison, includes several sequences from non-luminous species (*e.g., Pinnigorgia flava* (Nutting, 1910) and *Sinularia cruciata* (Tixier-Durivault, 1970)), in addition to several sequences from both our model species. Clade C also contained *the R*Luc-like enzymes retrieved from each transcriptome.

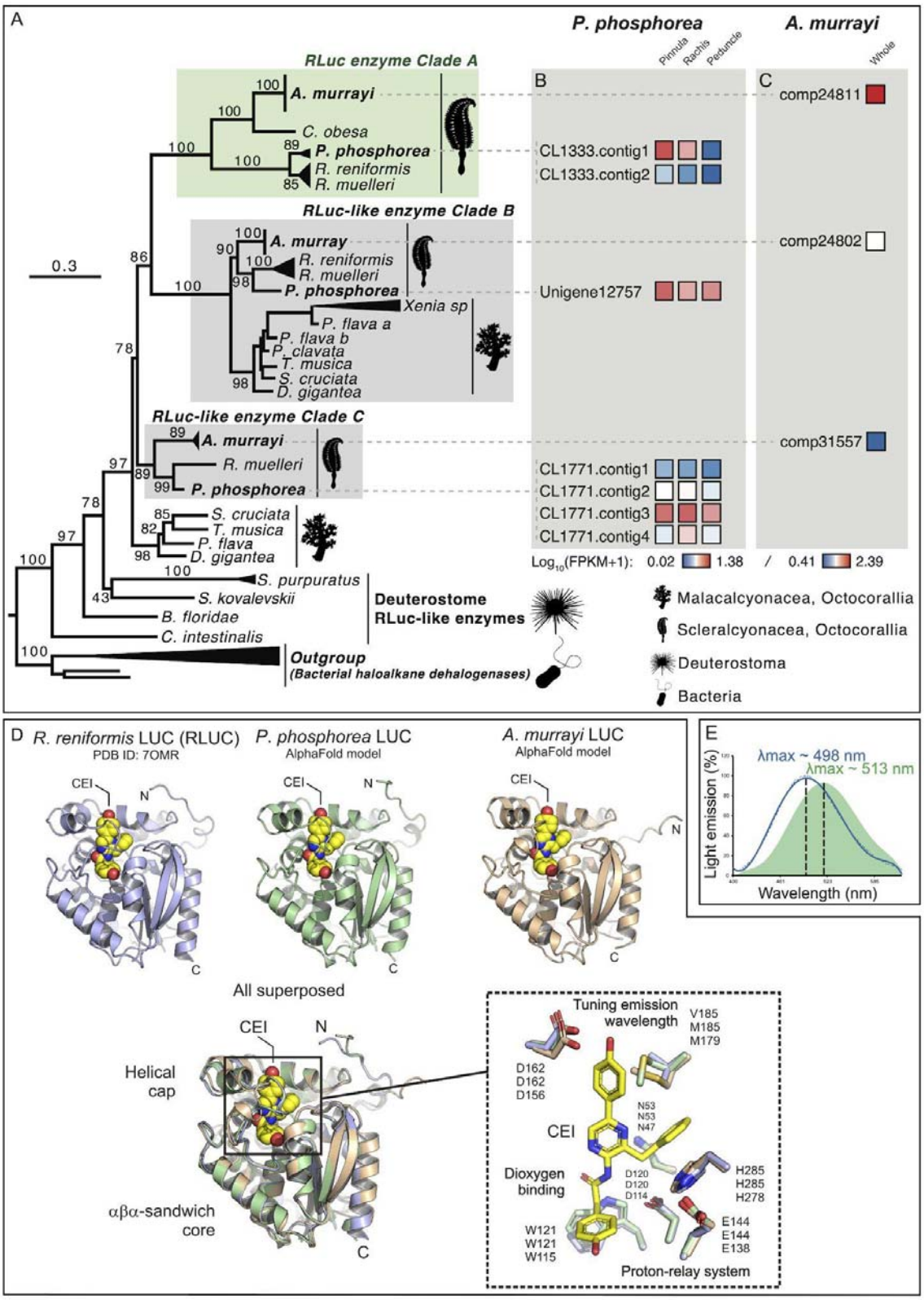

Figure 4. Phylogenetic tree of *R*Luc-like enzymes, including *P. phosphorea* and *A. murrayi* amino acid sequences. (A) Maximum likelihood tree based on the amino acid sequence alignment of *R*Luc-like enzymes. The tree was calculated by the IQ-tree software using the LG+I+G4 model of evolution. Numbers at the nodes indicate ultrafast bootstrap values based on 1000 replicates. The scale bar represents the percentage of amino

acid substitutions per site. Bacterial haloalkane dehalogenase sequences were used to root the tree. (B) The expression level of each retrieved *R*Luc-like sequence in a distinct portion of *P. phosphorea*. (C) Expression level of each retrieved *R*Luc-like sequence in *the whole A. murrayi* specimen. (D) Structural comparison of AlphaFold models of *P. phosphorea* and *A. murrayi* Luc proteins and the crystal structure of *R. reniformis* Luc complexes with coelenteramide (CEI) oxyluciferin (PDB ID: 7OMR). (E) Superimposed spectrum of the *in vivo* luminescence of *A. murrayi* (green) and the *in vitro* luminescent assay of *A. murrayi* luciferase in the presence of coelenterazine (fc.: 6 µM) (blue).

The retrieved sequence (CL1333; **Figure 4B**) of *P. phosphorea* luciferase has an estimated molecular weight of 35.84 kDa. A comparison of the amino acid sequences of *P. phosphorea* and anthozoan luciferases demonstrated the presence of the catalytic triad involved in luciferase activity. These key sites consist of an aspartate residue in position 120, a glutamate residue in position 144, and a histidine in position 285. The retrieved *P. phosphorea* luciferase sequence, based on RNA-seq data, appears to be highly similar to other known anthozoan luciferases. It shares 90.26% identity and 95% similarity with *Renilla reniformis* luciferase (*Renilla*-luciferin 2-monooxygenase). This sequence was validated by DNA amplification and sequencing using *R*Luc primers. FPKM analyses revealed that this sequence was mostly expressed in the pinnule and rachis (**Figure 4B**).

The *A. murrayi* luciferase (Comp24811, **Figure 4C**), with a molecular weight estimated at 34.61 kDa and consisting of 304 amino acids, exhibits 58% sequence identity and 98% coverage compared to *R*Luc, highlighting significant similarities. Sequence alignment of *A. murrayi* luciferase with *R*Luc has revealed the conservation of the catalytic triad and active site. The *R*Luc structure features two distinct domains: a cap domain and alpha/beta-hydrolase domain. Key residues essential for enzymatic activity, including the substrate entry tunnel and catalytic triad (D120, E144, and H285), are located in the cap domain. These elements have also been identified in the luciferase sequence of *A. murrayi*, as reported by Rahnama et al., 2017 [59] and Khoshnevisan et al. 2018 [60] for *Renilla* luciferase. Through the expression of recombinant luciferase in *Escherichia coli* using degenerate primers derived from *A. murrayi* transcriptome analysis, *A. murrayi* luciferase was tested for preliminary downstream expression, yielding an active enzyme capable of producing blue light (λmax = 498 nm) upon coelenterazine addition (**Figure 4E**).

Structural models of *P. phosphorea* and *A. murrayi* LUCs show a canonical aba-sandwich fold with a helical cap domain (**Figure 4D**). Overall comparison between the crystal structure of *R. reniformis* LUC complexed with coelenteramide (CEI) oxyluciferin and structural models of *P. phosphorea* and *A. murrayi* LUCs showed root-mean-square deviation (RMSD) on the C_a-atoms of 0.7 and 1.3, respectively. Careful inspection of the modeled LUC structures revealed that key residues of the catalytic pentad are conserved and properly positioned for productive catalysis (**Figure 4D**). From these, three residues (aspartate-histidine-glutamate) function as a protein-relay system protonating a CEI oxyluciferin at an amide nitrogen, while the two residues (asparagine and tryptophan) are responsible for co-substrate (dioxygen) binding. Moreover, an aspartate residue, responsible for tuning the

emission wavelength, found on the rim of the catalytic pocket in *R. reniformis* luciferase [13], is also conserved in these luminescent species.

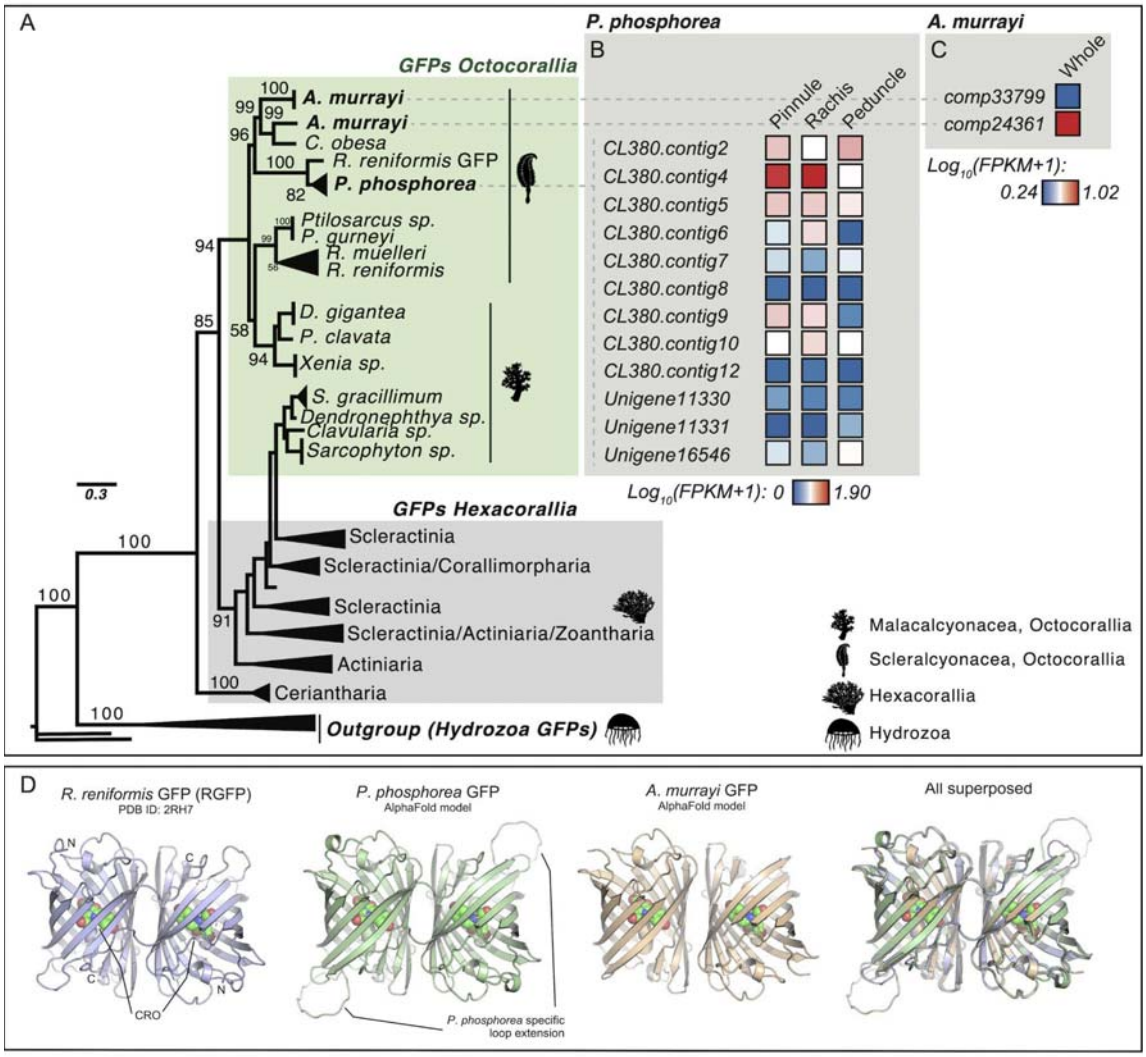

Figure 5. Phylogenetic tree of anthozoan fluorescent proteins, including *P. phosphorea* and *A. murrayi* amino acid sequences. (A) Maximum likelihood tree based on green fluorescent protein amino acid sequence alignment. The tree was calculated by the IQ-tree software using the WAG+R4 model of evolution. Numbers at the nodes indicate ultrafast bootstrap percentages based on 1,000 replicates. The scale bar represents the percentage of amino acid substitutions per site. Hydrozoan GFP sequences were used to root the tree. (B) The expression level of each retrieved CBP sequence for a distinct portion of *P. phosphorea*. (C) Expression level of each retrieved CBP sequence in *the whole A. murrayi* specimen. (D) Structural comparison of AlphaFold models of *P. phosphorea* and *A. murrayi* GFP proteins and the crystal structure of *R. reniformis* GFP (PDB ID: 2HR7).

Several sequences coding for GFP-like sequences were retrieved from *the P. phosphorea* and *A. murrayi* transcriptomes. *P. phosphorea* GFP (CL380; 20.81 kDa) and *A. murrayi* GFP (Comp24361; 27.24 kDa) appear homologous to other anthozoan sequences, and both sequences clustered with GFP sequences of bioluminescent Scleralcyonacea (**Figure 5A**). *P. phosphorea* GFP shares 79.42% identity and 86% similarity with the GFP of *R. reniformis*. In comparison, *A. murrayi* GFP shared 73.06% identity and 87% similarity with the GFP of

630 *Cavernularia obesa*. Pinnules and rachises were the main sites of P. phosphorea GFP
631 expression (**Figure 5B**). Among the unigene pairs found in the *A. murrayi* transcriptome,
632 Comp24361 appeared to be more highly expressed (**Figure 5C**).
633 Structural models of *P. phosphorea* and *A. murrayi* GFPs show a characteristic β-
634 barrel fold with a fluorophore moiety (CRO) covalently bound inside the barrel (**Figure 5D**).
635 *In silico* modeling suggests that these proteins may associate as homodimers, similar to the
636 homodimeric structure observed in the crystal structure of *R. reniformis* GFP. However,
637 further experimental validation is required to confirm this hypothesis. Comparison between
638 crystal structure of *R. reniformis* GFP and models of *P. phosphorea* and *A. murrayi* GFPs
639 showed RMSD on the C_a-atoms of 0.9 and 1.1, respectively, highlighting their high
640 similarities. A structural feature distinguishing *P. phosphorea* and *A. murrayi* GFPs from their
641 *R. reniformis* counterpart is the composition of the fluorophore moiety. While *R. reniformis*
642 fluorophore is generated from a serine-tyrosine-glycine tripeptide, the fluorophores of *P.*
643 *phosphorea* and *A. murrayi* are formed from a glutamine-tyrosine-glycine tripeptide, which
644 may affect the fluorescent properties of these proteins. Moreover, there is one markedly
645 extended solvent-exposed loop in *P. phosphorea* GFP (**Figure 5D**). We believe that this
646 species-specific extension might affecprotein t–protein complexation during the
647 radiationless resonance energy transfer process, but future experimental evidence is needed
648 to verify this hypothesis.
649

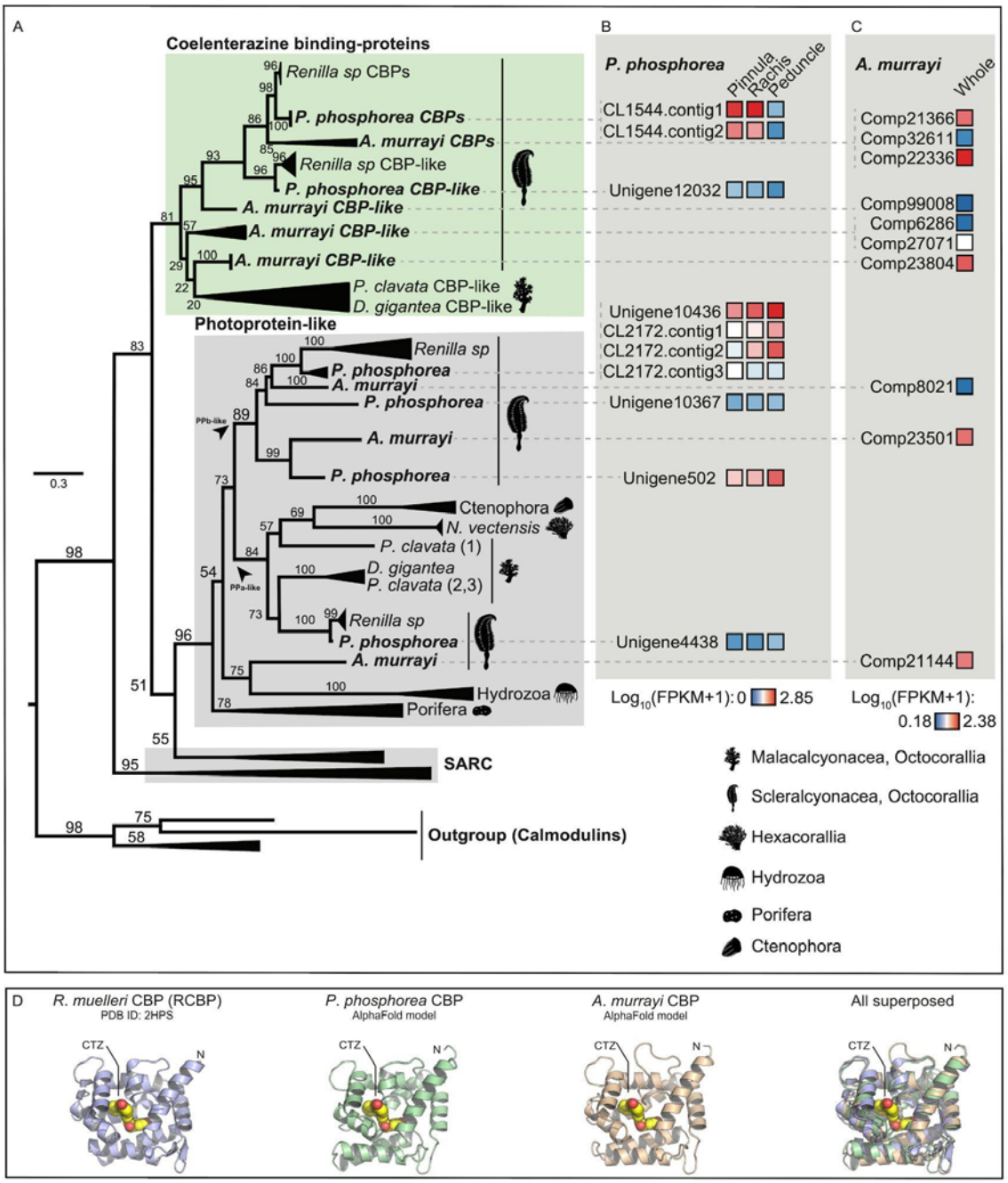

Figure 6. Phylogenetic tree of coelenterazine-binding proteins, including *P. phosphorea* and *A. murrayi* amino acid sequences. (A) Maximum likelihood tree based on the amino acid sequence alignment of coelenterazine-binding proteins. The tree was calculated by the IQ-tree software using the LG+R4 model of evolution. Numbers at the nodes indicate ultrafast bootstrap percentages based on 1000 replicates. The scale bar represents the percentage of amino acid substitutions per site. Calmodulin sequences were used to root the tree. (B) The expression level of each retrieved CBP sequence for a distinct portion of *P. phosphorea*. (C) Expression level of each retrieved CBP sequence in *the whole A. murrayi* specimen. (D) Structural comparison of AlphaFold models of *P. phosphorea* and *A. murrayi* CBP proteins and the crystal structure of *R. muelleri* CBP complexes with coelenterazine (CTZ) luciferin (PDB ID: 2HPS).

Different sequences of CBPs were retrieved from *the transcriptomes of P. phosphorea and A. murrayi*. Some of these sequences clustered with the CBPs of luminous Scleralcyonacea, whereas others were found to be clustered with photoprotein-like proteins (**Figure 6A**). One sequence appeared to be mainly expressed within the *P. phosphorea* pinnule and rachis (CL1544; 26.84 kDa) and *the A. murrayi* colony (Comp 22336; 21.08 kDa) (**Figure 6B, C**). The most highly expressed *P. phosphorea* CBP appeared highly similar to other luminous anthozoan sequences. *P. phosphorea* CBP shared 85.33% identity and 94% similarity with the luciferin-binding protein of *R. reniformis*, while *A. murrayi* CBP shared 50% identity and 74% similarity with the luciferin-binding of *R. reniformis*. Interestingly, sequences clustered in the photoprotein-like protein group appeared to be mainly expressed within the non-photogenic peduncle tissue in *P. phosphorea*.

Finally, structural models of *P. phosphorea* and *A. murrayi* Ca^{2+}-regulated CBPs reveal a typical EF-hand fold, containing three Ca^{2+}-binding sites. As shown in **Figure 6D**, comparison between the crystal structure of *R. reniformis* CBP complexed with coelenterazine (CTZ) luciferin and structural models of *P. phosphorea* and *A. murrayi* LUCs show a structural similarity, with RMSD on the C_a-atoms of 2.3 and 3.2, respectively. The RMSD values were higher than those observed for LUC and GFP proteins, but this is likely caused by a large conformational space that is searched by CBP proteins. Importantly, our modeling reveals an internal cavity in *P. phosphorea* and *A. murrayi* CBPs that is capable of accommodating CTZ luciferin, suggesting that these proteins are indeed functional luciferin-binding proteins (**Figure 6D**).

Luciferase expression and green autofluorescence in Pennatula phosphorea *and* Funiculina quadrangularis

Based on the high sequence similarity of *P. phosphorea* luciferase with *Renilla* luciferase, a commercial anti-Renilla luciferase antibody was selected for immunodetection. Immunoblot analyses revealed strong anti-luciferase immunoreactive bands in both extracts of the pinnule and rachis tissues (**Figure S3**). The bands correspond to a protein with an approximate molecular weight of 35 kDa, matching the molecular weight of the predicted *P. phosphorea* luciferase and the *Renilla* luciferase molecular weight of 36 kDa. No labeling was detected in the peduncle tissue extract (**Figure S3**).

On autozooid polyps of the pinnules (**Figure 7A-D**), a strong green autofluorescent signal was observed at the tentacle crown base before (**Figure 7B**) and after (**Figure 7C**) paraformaldehyde fixation. This fluorescent signal is located in clusters of cells at the tentacle junctions. Strong anti-*Renilla* luciferase immunoreactivity was observed at the same level as the green fluorescence signal (**Figure 7C, D**). On siphonozooid polyps of the rachis, the autofluorescent signal was also observable and was located as green dots (from 10 to 25 µm diameter) spread in the tissue, generally in pairs (**Figure 7E**). Anti-*Renilla* luciferase-positive cells colocalized with these autofluorescent dots (**Figure 7E, F**). Finally, no green fluorescence or immunolabeling was detected in peduncle tissue (data not shown).

For *Funiculina* polyps (**Figure 7G**), a green autofluorescent signal was observed in the freshly dissected specimens before fixation (**Figure 7H**). This green autofluorescence completely disappeared after fixation (**Figure 7I**). Luciferase localization differed from that in *P. phosphorea*. A strong luciferase signal was detected within the polyp tentacle tissue and not at the base of the polyp crown (**Figure 7I, J**).

Negative controls with the omission of the primary antibody did not reveal any non-specific binding of the secondary antibodies (data not shown).

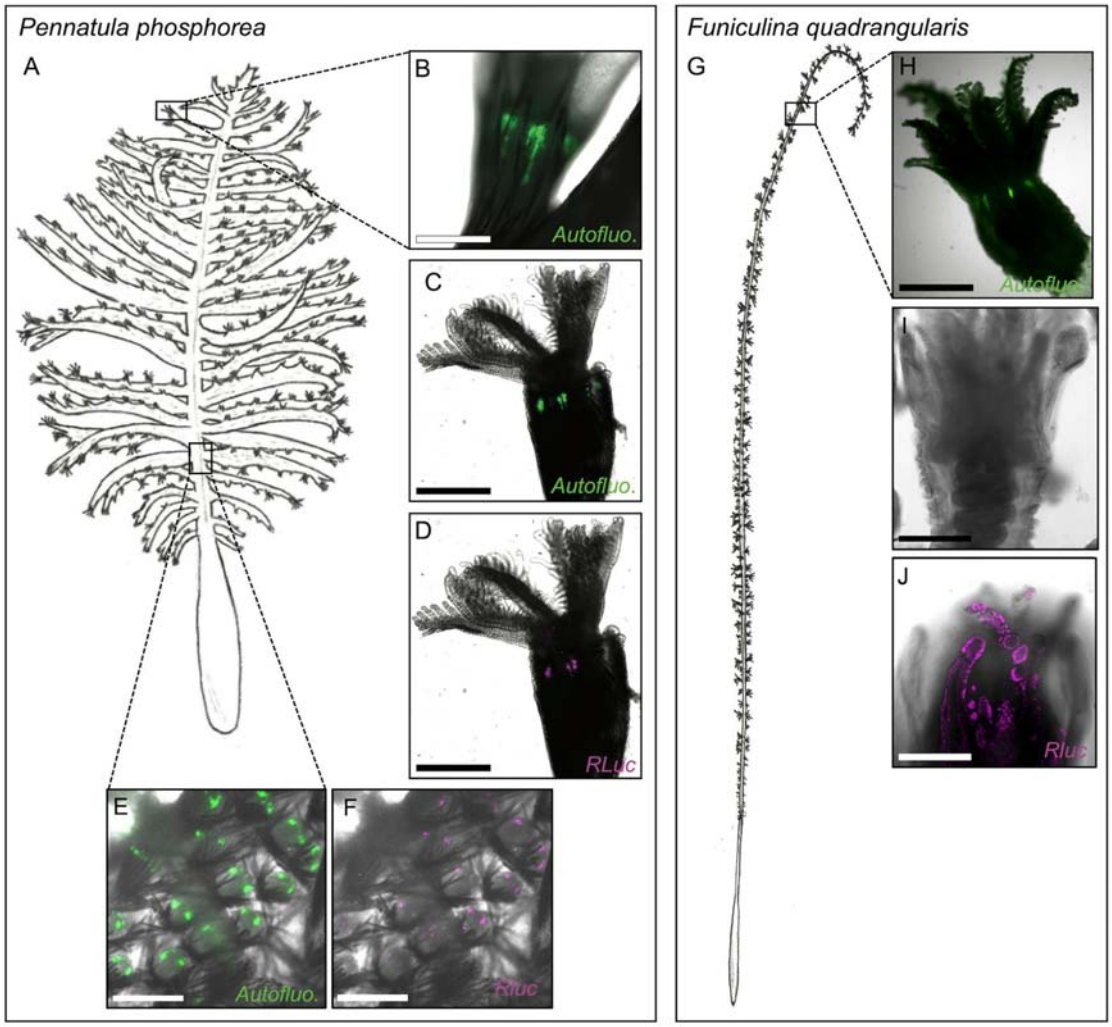

Figure 7. Autofluorescence and luciferase immunodetection in *P. phosphorea* and *F. quadrangularis*. (A) Schematic illustration of *P. phosphorea*. Natural green autofluorescence (B), green fluorescence after fixation (C), and luciferase immunodetection (D; magenta) of the *P. phosphorea* pinnule autozooids. Green fluorescence after fixation (E) and luciferase immunodetection (F; magenta) in *P. phosphorea* rachis siphonozooids. (G) Schematic illustration of *F. quadrangularis*. Natural green autofluorescence (H), observation after fixation with no autofluorescent signal (I), and luciferase immunodetection (J; magenta) of *the F. quadrangularis* autozooids. Scales: B-F, H - 500 µm; I, J - 250 µm.

Calcium is involved in the bioluminescence of Pennatula phosphorea *and* Funiculina quadrangularis

720
721 Based on *P. phosphorea* coelenterazine-binding protein retrieval in the *Pennatula*
722 transcriptome data and the literature mentioning the potential implication of Ca^{2+} in the
723 release of luciferin from coelenterazine-binding proteins, Ca^{2+} involvement in the light
724 emission process of *P. phosphorea* and *F. quadrangularis* was investigated. The tested
725 specimens of both species revealed a drastic increase in light production when immersed in
726 ASW with a doubled Ca^{2+} ion concentration (20 mM) (**Figure 8A, B**). At the same time, no
727 statistical differences were observed between the normal ASW (10 mM) and ASW devoted
728 to Ca^{2+} ions (0 mM) (**Figure 8A, B**). Analysis of the effects of the A23187 ionophore showed
729 no statistical differences compared to the calcium concentration (**Figure 8C, D**). For both
730 specimens, adrenaline triggered light production when calcium was present in ASW (**Figure**
731 **8E, F**). While an increase in the mean Ltot was observed between adrenaline tested samples
732 at 10 mM and 20 mM of $CaCl_2$ in the medium, this increase was not statistically supported
733 (**Figure 8E, F**). Finally, no significant differences were observed in Ltot after KCl application at
734 the three Ca^{2+} concentrations (**Figure S4**).
735

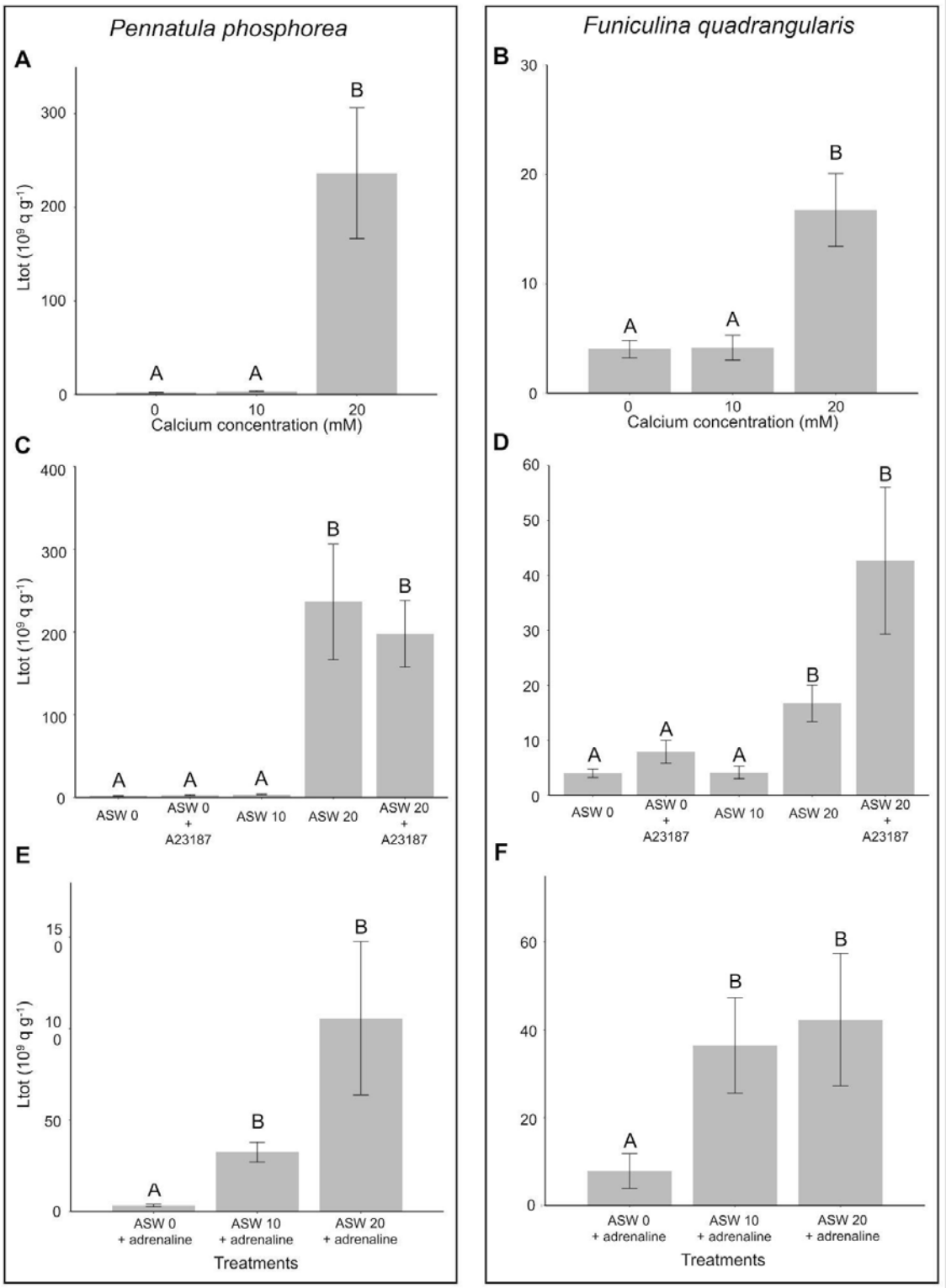

Figure 8. Calcium involvement in *P. phosphorea* and *F. quadrangularis* light emissions. Experiments were performed on *P. phosphorea* (A, C, E) and *F. quadrangularis* (B, D, F). Effect of different concentrations of calcium (0, 10, 20 mM) in the medium on the total light emission (Ltot) (A, B). Effect of different calcium concentrations (0, 10, 20 mM) in the medium in the presence and absence of the calcium ionophore A23187 on the Ltot (C, D). Effect of different concentrations of calcium (0, 10, 20 mM) in the medium in the presence of adrenaline (10^{-5} mol L^{-1}) on the Ltot (E, F). different lettering indicates statistical differences.

Discussion

Through biochemical cross-reaction experiments, this study demonstrated that the bioluminescence of *P. phosphorea*, *F. quadrangularis*, and *A. murrayi* is associated with a coelenterazine-dependent luciferase homologous to the well-known luciferase of the sea pansy *Renilla*. The measured concentration of coelenterazine in *P. phosphorea* pinnules closely aligns with the reported values of 141 and 282.4 ng g^{-1} for the phylogenetically closely related species *R. muelleri* and *C. obesa*, respectively [1]. Similarly, the mean luciferase activity of *P. phosphorea* pinnules reaches a comparable range as other organisms using *Renilla*-type luciferases such as *R. muelleri* (± 130 10^9 q g^{-1} s^{-1}) and *C. obesa* (± 220 10^9 q g^{-1} s^{-1}), or the sympatric ophiuroid *Amphiura filiformis* (± 69 10^9 q g^{-1} s^{-1}) [1,61]. While the luciferase activity recorded for *F. quadrangularis* is higher than *P. phosphorea*, this species exhibits a smaller coelenterazine content, being closer to recorded values of the echinoderms *A. filiformis* (5.4 ng g^{-1}; [61]) or the crinoid *Thalassometra gracilis* (Carpenter, 1888) (4.5 ng g^{-1}; [62]). Transcriptome and phylogenetic analyses confirm results for *P. phosphorea* and *A. murrayi* with a clear sequence conservation of the retrieved luciferases with the *Renilla* luciferase. Consistent with the literature, species such as *D. gracile* or undetermined species from the genera *Umbellula*, *Pennatula*, and *Funiculina* also present evidence of the use of coelenterazine as substrate and a *Renilla*-like luciferase as enzyme of their bioluminescent systems [12].

Our phylogenetic analysis underlines three distinctive clades of *Renilla*-like luciferase. One of these clades (Clade A) contains all the known sequences of anthozoan light-emitting luciferases. The other two clades (Clades B and C) contain other homologous *R*luc-like sequences, notably from non-luminous species. The related biochemical functionality and bioactivity of these B and C clades sequences are unknown and need further investigations to fully apprehend the evolution of luciferase among anthozoans. Nevertheless, this clustering led to hypothesized duplications of the ancestral gene with either (*i*) a neo functionality as a "real" functional luciferase able to catalyze a bioluminescent reaction or (*ii*) a bi-functionality of these enzymes as light-producing enzyme and another ancestrally conserved enzymatic function. The ancestral functionality of the *R*Luc enzyme has been assumed to originate from bacterial haloalkane dehalogenases, enzymes with a hydrolase activity cleaving bonds in halogenated compounds [63]. A basal gene transfer from bacteria until metazoans has been hypothesized [17,63]. Interestingly, *R*Luc-like luciferases have been demonstrated to be the enzymes involved in the bioluminescence of phylogenetically distinct species such as the brittle star *A. filiformis* [17] and the tunicate *P. atlanticum* (Péron, 1804) [18], letting assumed that the sequence was convergently coopted multiple times during the evolution. Consistent with previous research on *R*Luc sequences, our retrieved *P. phosphorea* and *A. murrayi* luciferase (Clade A) present high sequence similarity with the other pennatulaceans functional luciferases, also revealing conservation of the catalytic triads essential for the luciferase catalytic activity. The complete characterization of

P. phosphorea and *A. murrayi* luciferase will allow us to better apprehend the functionality and evolution of these luciferase enzymes.

While the retrieved GFP sequences are unique and well clustered with other Scleralcyonacea sequences, a similar observation, as for the luciferases, occurs for the CBPs with multiple retrieved sequences clustered in different groups. The first group represents the functional coelenterazine-binding protein retrieved and characterized in luminous species, while the second group, named photoprotein-like proteins, raise questions on the exact functionality of these retrieved sequences. These photoprotein-like proteins might also be involved in calcium binding. Active photoproteins of cnidarians and ctenophores depend on calcium to trigger light emission [64-67]. Nevertheless, the higher expression within the *P. phosphorea* peduncle assumed another function without a relationship with the bioluminescence.

AlphaFold is a neural network machine learning tool for predicting macromolecular structures and complexes, providing structural models with near-atomic accuracy even in the absence of known similar structures [68,69]. Here, we employed AlphaFold to predict macromolecular structures of the most expressed genes encoding for LUC, GFP, and CBP proteins in *P. phosphorea* and *A. murrayi*. Computational predictions yielded structural models with very high confidence scores (>90) for all analyzed proteins and that are structurally similar to crystallographic structures of well-characterized LUC [13], GFP [11], and CBP [70] proteins encoded by the sea pansies *R. reniformis* and *R. muelleri*. Taken together, our structural predictions suggest that the identified *P. phosphorea* and *A. murrayi* LUC, GFP, and CBP proteins with the highest expression values are structurally and functionally relevant and responsible for bioluminescence in these species.

Kept in captivity without exogenous coelenterazine supply, *P. phosphorea* can still produce light after one year, even if the coelenterazine content and luciferase activity decrease. Therefore, these results support a *de novo* synthesis of the coelenterazine substrate in *P. phosphorea*. Coelenterazine *de novo* synthesis by luminous marine organisms has been documented for the calanoid copepods *Metridia longa* (Lubbock, 1854) and *M. pacifica* (Brodsky, 1950), the oplophorid shrimp, *Systellaspis debilis* (Milne-Edwards, 1881), and two ctenophores, *Mnemiopsis leidyi* (Agassiz, 1865) and *Bolinopsis infundibulum* (Müller, 1776) [71-74]. The natural precursors of coelenterazine have been demonstrated to be the L-tyrosine and L-phenylalanine amino acids in *M. pacifica* [73]. By screening the transcriptomic data of 24 ctenophores, Francis et al., 2015, assumed the involvement of a non-heme iron oxidase-like enzyme, similar to isopenicillin-N-synthase, in the biosynthesis pathway of this luciferin [75]. Future research could be carried out to validate the *de novo* biosynthesis of the coelenterazine bioluminescent substrate, in particular by maintaining *P. phosphorea* and their offspring over generations in captivity in the same conditions without coelenterazine supply [74,76]. This protocol could be applied to other pennatulaceans to determine whether the coelenterazine genesis is a common trait in this clade. Nevertheless, the first challenge would be to control the life cycle of these species in captivity. Similarly, it would be interesting to analyze different pennatulacean transcriptomes searching for

enzymes homologous to the isopenicillin-N-synthase potentially involved in the coelenterazine biosynthetic pathway, as retrieved in ctenophores.

In *P. phosphorea*, the morphological localization of luciferase expression matched the green fluorescent sites obtained in unfixed and fixed tissues. Green autofluorescence observed on unfixed specimens is assumed to be a mix of the native autofluorescence of coelenterazine and the autofluorescent reaction occurring through the GFP, while green autofluorescence observed after tissue fixation corresponds only to the GFP signals. Comparatively, the *in vivo* green fluorescence observed in the *F. quadrangularis* tissues, which disappeared after fixation, was assumed to be related only to the natural autofluorescence of coelenterazine and the lack of GFP in this species. In contrast to *P. phosphorea,* which emits green waves of light at λmax = 510 nm, *F. quadrangularis* emits blue at λmax = 485 nm, supporting the absence of GFP for this species [12,34,58,77]. This natural autofluorescence has recently been demonstrated to appear and disappear from the photogenic site, depending on the substrate dietary acquisition of the brittle star *A. filiformis*. This species depends on the trophic acquisition of the coelenterazine substrate to produce light [61,78]. When the brittle star was fed with coelenterazine-containing food, green autofluorescent spots appeared at the level of spine-associated photocytes [78]. As for *F. quadrangularis*, a similar disappearance of the green fluorescent signal (possibly attributed to the coelenterazine) has been observed in the fixed tissue of the brittle star species [78]. The autofluorescent sites observed along the tentacle bases of the autozooids of *P. phosphorea* are consistent with the already described location of the autofluorescent photogenic cell processes in autozooids of *Stylatula elongata* [79], and to a lesser extent, *Acanthoptilum gracile,* and *Renilla koellikeri* [79,31]. For the former species, it was noticed that the photocytes process followed the same orientation as the longitudinal muscles, allowing autozooids to retract [31]. On the other hand, the luciferase expression site in *F. quadrangularis*, in the cellular processes of the apical part of the tentacle, was never reported before. This location along the polyp tentacles matches the described position of photocytes in autozooids of *Ptilosarcus* species [79].

Our spectrum measurement performed with the *A. murrayi* recombinant luciferase is consistent with already observed coelenterazine-dependent systems in other species emitting in the same range of wavelengths. Recorded spectrum for coelenterazine-dependent luciferase systems can vary between 475 to 493 nm in *P. atlanticum*, 482 nm emitted by *R*Luc, 472 nm emitted by the brittle star *A. filiformis*, 455 nm emitted by *Oplophorus gracilirostris* and 485 nm emitted by *F. quadrangularis* [17,18,63,80]. According to the natural spectrum recorded on the whole specimens (λmax = 513 nm), similar to the spectrum measured for *P. phosphorea* [58], and the transcriptomic presence of a GFP sequence in *A. murrayi*, this species is strongly assumed to display a GFP-associated coelenterazine-dependent luminous system. At least six anthozoan species present expression of a GFP and the production of green light. Some of these species may live in sympatry with anthozoan blue emitters, such as *P. phosphorea* and *F. quadrangularis,* with an overlap of depth repartition and habitat preferences occurring. Therefore, questions arise

concerning luminescence's exact function(s) among anthozoans. Even if some assumptions are proposed in the literature, no one has ever developed an ethological protocol to validate them [35]. Therefore, why some anthozoan evolved green light emission while the primary coelenterazine-luciferase reaction produces blue light remains. Different function(s) in the same environment may have led to the acquisition or the loss of the GFP gene by some anthozoan species upon evolutionary constraints.

As demonstrated for other pennatulacean species, CBP seems to be an essential component of the luminous system [19-23,25]. The retrieved CBPs in *P. phosphorea* and *A. murrayi* are congruent with this literature. Gene ontology distribution analyses performed on the different tissues of *P. phosphorea* underline a high expression of calcium ion binding proteins, including the retrieved CL1333 CBP, in the photogenic tissue (pinnule and rachis) of this species. The expression of this gene within the photogenic tissues supports its involvement in the luminous reaction. As demonstrated for *Renilla* by Stepanyuk et al., 2008, CBPs need calcium as a cofactor to release the coelenterazine [27]. In addition to the retrieved CBPs sequence in the *Pennatula* transcriptome, our calcium assay results highlight the involvement of the calcium ion in the light emission process of both *P. phosphorea* and *F. quadrangularis*. Results obtained for the calcium ionophore A23187 reveal that the ion action does not result from intracellular calcium storage but rather is provided by external calcium input. Moreover, calcium is shown to be essential for the physiological luminescent response through adrenaline application. Pieces of evidence of calcium involvement in anthozoan luminescence were already described for *R. reniformis* and *V. cynomorium* [25,26].

These results let us assume a conservation of the coelenterazine-dependent *Renilla*-like luciferase bioluminescent system, involving also a CBP, across luminous Pennatulaceans (**Table S1**). The involvement of GFP appears species-dependent, with only a few species emitting blue light (**Table S1**). Nevertheless, deeper investigations are needed to fully apprehend the conservation of those actors across the diversity of luminous pennatulaceans.

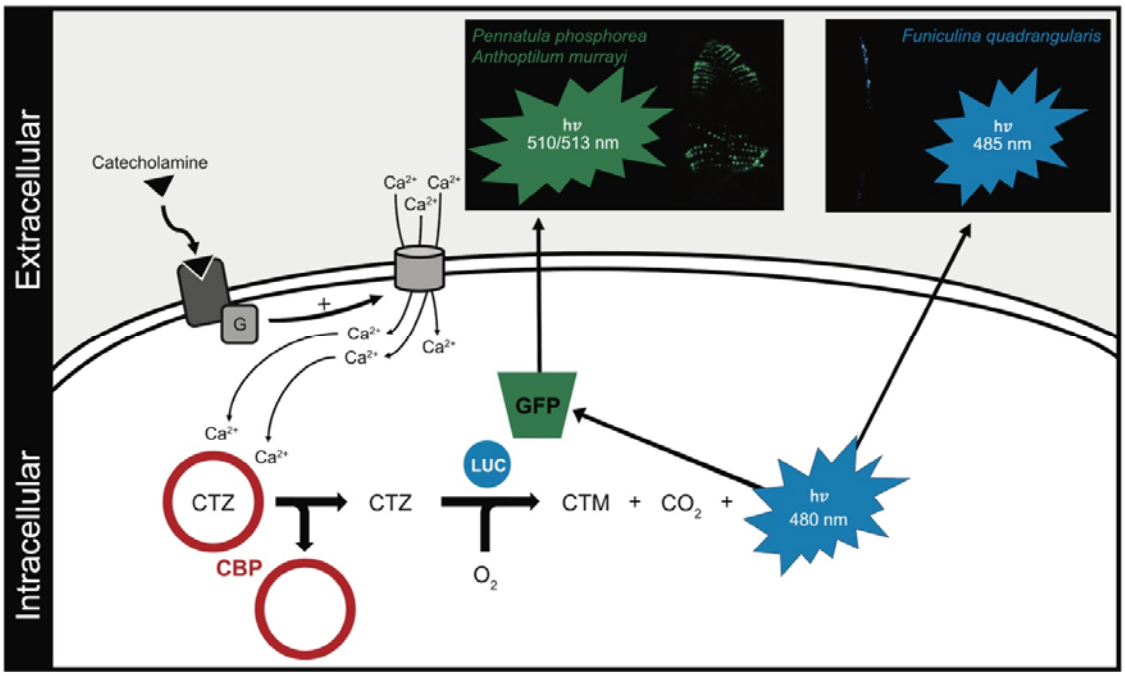

Figure 9: Schematic representation of the putative pathway driving the luminescence production in sea pens. Elements of this pathway have been compiled from the present results and the literature [12,13,16,19-23,30-34]. CBP, coelenterazine-binding protein; CTM, coelenteramide; CTZ, coelenterazine; G, G-protein; GFP, green fluorescent protein.

A hypothetical scheme of the generalized pathway could be established using our results and the literature on the pennatulacean luminescence mechanism (**Figure 9**). The first step is the activation of catecholaminergic receptors through the binding of biogenic amines (mainly adrenaline and noradrenaline [33,34]), which will release an intracellular-associated G-protein [81,82]. G-protein could be involved in a large variety of intracellular pathways [83], some of which involve increasing intracellular calcium (via direct or indirect activation of calcium channels) [84-87]. This intracellular calcium increase will lead to the release of the coelenterazine through the binding of this ion on the CBP, leaving this luciferin free to react with luciferase in the presence of oxygen to produce blue light around 480 nm [9,10,15,19-23,25]. For pennatulaceans lacking GFP (*e.g., F. quadrangularis*), this scheme ends here with the direct emission in blue color, while for those displaying GFP expression, the blue light is captured by this specific fluorescent protein and reemitted in green wavelength [20], such as for *P. phosphorea*. Future research is needed to validate this hypothetical scheme, and further investigations will be conducted to establish the functional activities of all these components in less-studied sea pens. Astonishingly, even if attempts were made on other anthozoans over the past decades, the *Renilla* bioluminescence system remains the only isolated and cloned system [13,15,20-23,25]. Despite the demonstrated widespread uses of the sea pansy bioluminescent system in biotechnology and biomedicine [*e.g.,* 88-90], the *Renilla* luciferase stands as the only one of the most commercially employed gene reporters in biomolecular sciences. Nonetheless, in the *Renilla*

bioluminescence system, the exact action mode of CBP and calcium is not fully apprehended. Considering these facts, our introspection into the bioluminescent system of other luminous pennatulaceans could be of great use for new biotechnological advances. Our results provided a better understanding of the evolution of the bioluminescence system and associated molecules from these enigmatic benthic sessile organisms.

Supplemental data captions

Table S1. General overview of the bioluminescent knowledge among luminous anthozoans. All data were extracted from the literature (only scientific data described for species down to the species level have been taken into account to minimize generalizations). CBP, coelenterazine-binding protein; GFP, green fluorescent protein.

Table S2. Primers designed for *P. phosphorea* luciferase validation.

Table S3. Experiment protocol for the calcium assays.

Table S4. Description of the output sequenced data. Q20 percentage is the proportion of nucleotides with a quality value larger than 20 in reads. GC percentage is the proportion of guanidine and cytosine nucleotides among total nucleotides.

Table S5. Summary statistics of assemblies for *Pennatula phosphorea* pinnules, rachis, peduncle, and *Anthoptilum murrayi* transcriptomes.

Table S6. Transcript expression values (FPKM values) and public database sequences used during transcriptomic and phylogenetic analyses.

Figure S1: Luminometric measurements performed on the different area of *Pennatula phosphorea*. (A) schematic representation of *P. phosphorea* with the different areas (upper, middle, lower) of the pinnules and rachis. (B) Mean coelenterazine content recorded and (C) luciferase activity for the different pinnule areas. (D) Mean coelenterazine content recorded and (E) luciferase activity for the different rachis areas.

Figure S2: Biochemical assays following luminous parameters activity on *Pennatula phosphorea* pinnules (A, B, C) and rachis (D, E, F) during 1 year without coelenterazine supply. Mean total light emission after KCl applications (A, D), mean coelenterazine content (B, E), and mean maximal light emission during luciferase activity experiments (C, D). Different lettering indicates statistical differences. The timing corresponds to experiments performed on wild-caught specimens (T0) after 6 months (T6) and twelve months of captivity (T12).

Figure S3. Luciferase immunoblots on *Pennatula phosphorea* tissues (rachis, Ra; peduncle, Ped; and pinnule, Pin).

964 **Figure S4. Total light emission (Ltot) after KCl applications with three different calcium**
965 **concentrations in the medium.** Experiments were performed on (A) pinnules, and (B) rachis of
966 *Pennatula phosphorea*. ASW, artificial seawater; 0, 10, 20 correspond to the calcium concentration
967 (mM) in the medium.
968
969 **Acknowledgment**
970 The authors acknowledge U. Schwarz, captain of the Alice vessel, and the skillful members of
971 the Kristineberg Center (Goteborg University, Sweden) for their help during the *Pennatula*
972 and *Funiculina* collection; and commandant J. Rezende and the crew of the R/V Alpha Crucis
973 (Instituto Oceanográfico, USP). The authors also thank M. Jacquet for contributing to the
974 study during his master's thesis and C. Pels, ELIV laboratory technician who maintained the
975 organisms in the aquaria at the Marine Biology Laboratory - UCLouvain. The authors also
976 want to thank T. Wiegand from the mobile lab (TREC- EMBL) for her help in visualizing
977 coelenterazine autofluorescence and immunolabeling in the wild-caught specimens. The
978 authors also thank J. Mallefet for his helpful advice and help during the first organisms
979 sampling and all along the experiments.
980 LD is a postdoctoral researcher at the Université de Louvain - UCLouvain, GG is a
981 Ph.D. student at Universidade de São Paulo - USP, CC is a Ph.D. student under an FRIA
982 fellowship, LB is a postdoctoral researcher at the Université de Louvain - UCLouvain, RR is an
983 academic professor at UCLouvain, MRSM is an academic professor at Universidade de São
984 Paulo - USP, MM is group leader at the Masaryk University, DTA is adjunct professor at
985 Federal University of ABC, SD is a Senior Lecturer and Associate professor at the University
986 of Gothenburg, AGO is an assistant professor at Yeshiva University, and JD is a postdoctoral
987 researcher at FNRS. This study is the contribution of BRC#422 of the Biodiversity Research
988 Center (UCLouvain) from the Earth and Life Institute Biodiversity (ELIV) and the "Centre
989 Interuniversitaire de Biologie Marine" (CIBIM).
990
991 **Competing interests**
992 No competing interests declared
993
994 **Data availability**
995 Transcriptome raw reads were uploaded as Sequence Reads Archives (SRA): *A. murrayi*
996 (PRJNA1144931), *P. phosphorea* (PRJNA1152785). The unigene annotation tables are
997 accessible from the corresponding author upon request.
998
999 **Funding**
1000 This work was supported by an F.R.S.-FNRS grant (T.0169.20) awarded to the Université de
1001 Louvain – UCLouvain Marine Biology Laboratory and the Université de Mons Biology of
1002 Marine Organisms and Biomimetics Laboratory, by the Czech Science Foundation (GA22-
1003 09853S), and by the Czech Ministry of Education, Youth and Sports (RECETOX RI LM2023069,
1004 e-INFRA LM2018140). The research leading to these results also received funding from the
1005 European Union's Horizon 2020 research and innovation program under grant agreement

No 730984, ASSEMBLE Plus project. This study was financed in part by the Coordenação de Aperfeiçoamento de Pessoal de Nível Superior - Brasil (CAPES) - Finance Code 88887.605088/2021-00; Fundação de Amparo à Pesquisa do Estado de São Paulo (FAPESP 2017/12909-4, 2020/07600-7), and Yeshiva University Start-up Fund..

Author contributions

LD, CC, and SD collected the *P. phosphorea* and *F. quadrangularis* samples, and GG and MRSM sampled *A. murrayi*. Data collection and analyses were performed by LD, CC, LB, GG, AO and JD. Transcriptome analyses were performed by LD, GG, DTA, AO, and JD. Phylogenetic analyses were performed by JD. Structural analyses were performed by MM. The project was supervised by RR, SD, AO, and JD. The original manuscript was written by LD, GG, CC, AO, and JD. All the authors reviewed and approved the final version.

Reference

1. Shimomura O, Yampolsky IV. 2019 *Bioluminescence: chemical principles and methods*. 3rd edition (Singapore: World Scientific Publishing), 1–556.
2. Haddock SHD, Moline MA, Case JF. 2010 Bioluminescence in the sea. *Ann. Rev. Mar. Sci.* **2**, 443-493. (https://doi.org/10.1146/annurev-marine-120308-081028)
3. Delroisse J, Duchatelet L, Flammang P, Mallefet J. 2021 Leaving the dark side? Insights into the evolution of luciferases. *Front. Mar. Sci.* **8**, 673620. (https://doi.org/10.3389/fmars.2021.673620)
4. Fleiss A, Sarkisyan KS. 2019 A brief review of bioluminescent systems. *Curr. Genet.* **65**, 877-882. (https://doi.org/10.1007/s00294-019-00951-5)
5. Hastings JW. 1996 Chemistries and colors of bioluminescent reactions: a review. *Gene* **173(1)**, 5-11. (https://doi.org/10.1016/0378-1119(95)00676-1)
6. Wilson T, Hastings JW. 2012 *Bioluminescence: living lights, lights for living*. Harvard University Press.
7. Kaskova ZM, Tsarkova AS, Yampolsky IV. 2016 1001 lights: luciferins, luciferases, their mechanisms of action and applications in chemical analysis, biology and medicine. *Chem. Soc. Rev.* **45**, 6048-6077. (https://doi.org/10.1039/C6CS00296J)
8. Cormier MJ. 1960 Studies of the bioluminescence of *Renilla reniformis*: I. Requirements for luminescence in extracts and characteristics of the system. *Biochimica et Biophysica Acta* **42**, 333-343. (https://doi.org/10.1016/0006-3002(60)90797-6)
9. Matthews JC, Hori K, Cormier MJ. 1977 Purification and properties of *Renilla reniformis* luciferase. *Biochemistry* **16(1)**, 85-91. (https://doi.org/10.1021/bi00620a014)
10. Lorenz WW, McCann RO, Longiaru M, Cormier MJ. 1991 Isolation and expression of a cDNA encoding *Renilla reniformis* luciferase. *PNAS* **88(10)**, 4438-4442. (https://doi.org/10.1073/pnas.88.10.4438)
11. Loening AM, Fenn TD, Gambhir SS. 2007 Crystal structures of the luciferase and green fluorescent protein from *Renilla reniformis*. *J. Mol. Biol.* **374(4)**, 1017-1028. (https://doi.org/10.1016/j.jmb.2007.09.078)

12. Bessho-Uehara M, Francis WR, Haddock SHD. 2020 Biochemical characterization of diverse deep-sea anthozoan bioluminescence systems. *Mar. Biol.* **167**, 114. (https://doi.org/10.1007/s00227-020-03706-w)
13. Schenkmayerova A, Toul M, Pluskal D, Baatallah R, Gagnot G, Pinto GP, Santana VT, et al. 2023 Catalytic mechanism for *Renilla*-type luciferases. *Nat. Catal.* **6**, 23-38. (https://doi.org/10.1038/s41929-022-00895-z)
14. DeLeo D, Bessho-Uehara M, Haddock SHD, McFadden CS, Quattrini AM. 2024 Evolution of bioluminescence in Anthozoa with emphasis on Octocorallia. *Proc. R. Soc. B.* **291**, 20232626. (https://doi.org/10.1098/rspb.2023.2626)
15. Inoue S, Kakoi H, Murata M, Goto T, Shimomura O. 1977 Complete structure of *Renilla* luciferin and luciferyl sulfate. *Tetrahedron Lett.* **18(31)**, 2685-2688. (https://doi.org/10.1016/S0040-4039(01)83046-X)
16. Cormier MJ, Hori K, Karkhanis YD, Anderson JM, Wampler JE, Morin JG, Hastings JW. 1973 Evidence for similar biochemical requirements for bioluminescence among coelenterates. *J. Cell. Physiol.* **81(2)**, 291-297. (https://doi.org/10.1002/jcp.1040810218)
17. Delroisse J, Ullrich-Lüter E, Blaue S, Ortega-Martinez O, Eeckhaut I, Flammang P, Mallefet J. 2017 A puzzling homology: a brittle star using a putative cnidarian-type luciferase for bioluminescence. *Open Biol.* **7(4)**, 160300. (https://doi.org/10.1098/rsob.160300)
18. Tessler M, Gaffney JP, Oliveira AG, Guarnaccia A, Dobi KC, Gujarati NA, et al. 2020 A putative chordate luciferase from a cosmopolitan tunicate indicates convergent bioluminescence evolution across phyla. *Sci. Rep.* **10**, 17724. (https://doi.org/10.1038/s41598-020-54373446-w)
19. Anderson J, Charbonneau H, Cormier MJ. 1974 Mechanism of calcium induction of *Renilla* bioluminescence. Involvement of a calcium-triggered luciferin binding protein. *Biochemistry* **13(6)**, 1195-1200. (https://doi.org/10.1021/bi00703a602)
20. Ward WW, Cormier MJ. 1979 Energy transfer protein in coelenterate bioluminescence. Characterization of the *Renilla* green-fluorescent protein. *J. Biol. Chem.* **254(3)**, 781-788.
21. Kumar S, Harrylock M, Walsh KA, Cormier MJ, Charbonneau H. 1990 Amino acid sequence of the Ca^{2+}-triggered luciferin binding protein of *Renilla reniformis*. *FEBS Lett.* **268(1)**, 287-290. (https://doi.org/10.1016/0014-5793(90)81029-N)
22. Inouye S. 2007 Expression, purification and characterization of calcium-triggered luciferin-binding protein of *Renilla reniformis*. *Protein Expr. Purif.* **52(1)**, 66-73. (https://doi.org/10.1016/j.pep.2006.07.028)
23. Titushin MS, Markova SV, Frank LA, Malikova NP, Stepanyuk GA, Lee J, Vysotski ES. 2008 Coelenterazine-binding protein of *Renilla muelleri* : cDNA cloning, overexpression, and characterization as a substrate of luciferase. *Photochem. Photobiol. Sci.* **7**, 189-196. (https://doi.org/10.1039/b713109g)

24. Ogoh K, Kinebuchi T, Murai M, Takahashi T, Ohmiya Y, Suzuki H. 2013 Dual-color-emitting green fluorescent protein from the sea cactus *Cavernularia obesa* and its use as a pH indicator for fluorescent microscopy. *Luminescence* **28(4)**, 582-591. (https://doi.org/10.1002/bio.2497)
25. Henry J-P, Ninio M. 1978 Control of the Ca^{2+}-triggered bioluminescence of *Veretillum cynomorium* lumisomes. *Biochimica et Biophysica acta* **504(1)**, 40-59. (https://doi.org/10.1016/0005-2728(78)90005-1)
26. Charbonneau H, Cormier MJ. 1979 Ca^{2+}-induced bioluminescence in *Renilla reniformis*. Purification and characterization of a calcium-triggered luciferin-binding protein. *J. Biol. Chem.* **254(3)**, 769-780. (https://doi.org/10.1016/S0021-9258(17)37872-9)
27. Stepanyuk GA, Liu Z-J, Vysotski ES, Lee J, Rose JP, Wang B-C. 2008 Structure based mechanism of the Ca^{2+}-induced release of coelenterazine from the *Renilla* binding protein. *Proteins* **74(3)**, 583-593. (https://doi.org/10.1002/prot.22173)
28. Nicol JAC. 1955 Observations on luminescence in *Renilla* (Pennatulacea). *J. Exp. Biol.* **51232(2)**, 299-320.
29. Davenport D, Nicol JAC. 1956 Observations on luminescence in sea pens (Pennatulacea). *Proc. R. Soc. B* **144(917)**, 480-496. (https://doi.org/10.1098/rspb.1956.0005)
30. Wampler JE, Karkhanis YD, Morin JG, Cormier MJ. 1973 Similarities in the bioluminescence from the Pennatulacea. *Biochimica et Biophysica Acta* **314**, 104-109. (https://doi.org/10.1016/0005-2728(73)90068-6)
31. Satterlie RA, Anderson PAV, Case JF. 1980 Colonial coordination on anthozoans: Pennatulacea. *Mar. Behav. Physiol.* **7**, 25-46. (https://doi.org/10.1080/10236248009386969)
32. Germain G, Anctil M. 1988 Luminescent activity and ultrastructural characterization of photocytes dissociated from the coelenterate *Renilla köllikeri*. *Tissue and Cell* **20(5)**, 701-720. (https://doi.org/10.1016/0040-8166(88)90017-1)
33. Anctil M, Boulay D, Larivière L. 1982 Monoaminergic mechanisms associated with control of luminescence and contractile activities in the coelenterate, *Renilla köllikeri*. *J. Exp. Zool.* **223(1)**, 11-24. (https://doi.org/10.1002/jez.1402230103)
34. Duchatelet L, Coubris C, Pels C, Dupont S, Mallefet J. 2023 Catecholamine involvement in the bioluminescence control of two species of Anthozoans. *Life* **13(9)**, 1798. (https://doi.org/10.3390/life13091798)
35. Morin JG. 1976 Probable functions of bioluminescence in the Pennatulacea (Cnidaria, Anthozoa). In: Mackie GO. (Ed) *Coelenterate Ecology and Behavior*. Springer, Boston, MA, USA. (https://doi.org/10.1007/978-1-4757-9724-4_65)
36. Delroisse J, Mallefet J, Flammang P. 2016 *De novo* adult transcriptomes of two European brittle stars: spotlight on opsin-based photoreception. *PLoS ONE* **11(4)**, e0152988. (https://doi.org/10.1371/journal.pone.0152988)
37. Delroisse J, Duchatelet L, Flammang P, Mallefet J. 2018 *De novo* transcriptome analyses provide insights into opsin-based photoreception in the lanternshark

Etmopterus spinax. *PLoS ONE* **13(12)**, e0209767. (https://doi.org/10.1371/journal.pone.0209767)

38. Delroisse J, Duchatelet L, Flammang P, Mallefet J. 2021 Photophore distribution and enzymatic diversity within the photogenic integument of the cookie-cutter shark *Isistius brasiliensis* (Chondrichthyes: Dalatiidae). *Front. Mar. Sci.* **8**, 627045. (https://doi.org/10.3389/fmars.2021.627045)
39. Cock PJA, Fields CJ, Goto N, Heuer ML, Rice PM. 2010 The Sanger FASTQ file format for sequences with quality scores and the Solexa/Illumina FASTQ variants. *Nucleic Acids Res.* **38(6)**, 1767-1771. (https://doi.org/10.1093/nar/gkp1137)
40. Grabherr MG, Haas BJ, Yassour M, Levin JZ, Thompson DA, Amit I, et al. 2011 Full-length transcriptome assembly from RNA-Seq data without a reference genome. *Nat. Biotechnol.* **29**, 644-652. (https://doi.org/10.1038/nbt.1883)
41. Pertea G, Huang X, Liang F, Antonescu V, Sultana R, Karamycheva S, et al. 2002 TIGR gene indices clustering tools (TGICL): a software system for fast clustering of large EST datasets. *Bioinformatics* **19(5)**, 651-652. (https://doi.org/10.1093/bioinformatics/btg034)
42. Das S, Shyamal S, Durica DS. 2016 Analysis of annotation and differential expression methods used in RNA-seq studies in crustacean systems. *Integr. Comp. Biol.* **56(6)**, 1067-1079. (https://doi.org/10.1093/icb/icw117)
43. Altschul SF, Gish W, Miller W, Myers EW, Lipman DJ. 1990 Basic local alignment search tool. *J. Mol. Biol.* **215(3)**, 403-410. (https://doi.org/10.1016/S0022-2836(05)80360-2)
44. Buchfink B, Xie C, Huson DH. 2014 Fast and sensitive protein alignment using DIAMOND. *Nat. Methods* **12**, 59-60. (https://doi.org/10.1038/nmeth.3176)
45. Conesa A, Götz S, García-Gómez JM, Terol J, Talón M, Robles M. 2005 Blast2GO: a universal tool for annotation, visualization and analysis in functional genomics research. *Bioinformatics* **21(18)**, 3674-3676. (https://doi.org/10.1093/bioinformatics/bti610)
46. Quevillon E, Silventoinen V, Pillai S, Harte N, Mulder N, Apweiler R, Lopez R. 2005 InterProScan: protein domains identifier. *Nucleic Acids Res.* **33**, W116-W120. (https://doi.org/10.1093/nar/gki442)
47. Kearse M, Moir R, Wilson A, Stones-Havas S, Cheung M, Sturrock S, et al. 2012 Geneious Basic: an integrated and extendable desktop software platform for the organization and analysis of sequence data. *Bioinformatics* **28(12)**, 1647-1649. (https://doi.org/10.1093/bioinformatics/bts199)
48. Woo J, Howell MH, von Arnim AG. 2009 Structure-function studies on the active site of the coelenterazine-dependent luciferase from *Renilla*. *Protein Sci.* **17(4)**, 725-735. (https://doi.org/10.1110/ps.073355508)
49. McFadden CS, van Ofwegen LP, Quattrini AM. 2022 Revisionary systematics of Octocorallia (Cnidaria: Anthozoa) guided by phylogenomics. *Bulletin of the Society of Systematics Biologists* **1(3)**. (https://doi.org/10.18061/bssb.v1i3.8735)

50. Labas YA, Gurskaya NG, Yanushevich YG, Fradkov AF, Lukyanov KA, Lukyanov SA, Matz MV. 2002 Diversity and evolution of the green fluorescent protein family. *Proc. Natl Acad. Sci.* **99(7)**, 4257-4261. (https://doi.org/10.1073/pnas.062552299)
51. Alieva NO, Konzen KA, Field SF, Meleshkevitch EA, Hunt ME, Beltran-Ramirez V, Miller DJ, Wiedenmann J, Salih A, Matz MV. 2008 Diversity and evolution of coral fluorescent proteins. *PLoS ONE* **3(7)**, e2680. (https://doi.org/10.1371/journal.pone.0002680)
52. Li G, Zhang QJ, Zhong J, Wang YQ. 2009 Evolutionary and functional diversity of green fluorescent proteins in cephalochordates. *Gene* **446(1)**, 41-49. (https://doi.org/10.1016/j.gene.2009.07.003)
53. Shagin DA, Barsova EV, Yanushevich YG, Fradkov AF, Lukyanov KA, Labas YA, Semenova TN, Ugalde JA, Meyers A, Nunez JM, Widder EA, Lukyanov SA, Matz MV. 2004 GFP-like proteins as ubiquitous metazoan superfamily: evolution of functional features and structural complexity. *Mol. Biol. Evol.* **21(5)**, 841-850. (https://doi.org/10.1093/molbev/msh079)
54. Schnitzler CE, Pang K, Powers ML, Reitzel AM, Ryan JF, Simmons D, Tada T, Park M, Gupta J, Brooks SY, Blakesley RW, Yokoyama S, Haddock SHD, Martindale MQ, Baxevanis AD. 2012 Genomic organization, evolution, and expression of photoprotein and opsin genes in *Mnemiopsis leidyi*: a new view of ctenophore photocytes. *BMC Biol.* **10**, 1-26. (https://doi.org/10.1186/1741-7007-10-107)
55. Capella-Gutierrez S, Silla-Martinez JM, Gabaldon T. 2009 trimAl: a tool for automated alignment trimming in large-scale phylogenetic analyses. *Bioinformatics* **25**, 1972-1973. (https://doi.org/10.1093/bioinformatics/btp348)
56. Nguyen LT, Schmidt HA, Von Haeseler A, Minh BQ. 2015 IQ-TREE: a fast and effective stochastic algorithm for estimating maximum-likelihood phylogenies. *Mol. Biol. Evol.* **32(1)**, 268-274. (https://doi.org/10.1093/molbev/msu300)
57. Posada D, Crandall KA. 1998 MODELTEST: testing the model of DNA substitution. *Bioinformatics (Oxford, England)* **14(9)**, 817-818. (https://doi.org/10.1093/bioinformatics/14.9.817)
58. Nicol JAC. 1958 Observations on the luminescence of *Pennatula phosphorea*, with a note on the luminescence of *Virgularia mirabilis*. *J. Mar. Biol. Assoc. UK* **37**, 551–563. (https://doi.org/10.1017/S0025315400005610)
59. Rahnama S, Saffar B, Kahrani Z.F, Nazari M, Emamzadeh R. 2017 Super RLuc8: a novel engineered *Renilla* luciferase with a red-shifted spectrum and stable light emission. *Enzym. Microb. Technol.* **96**, 60-66. (https://doi.org/10.1016/j.enzmictec.2016.09.009)
60. Khoshnevisan G, Emamzadeh R, Nazari M, Rasa SMM, Sariri R, Hassani L. 2018 Kinetics, structure, and dynamics of *Renilla* luciferase solvated in binary mixtures of glycerol and water and the mechanism by which glycerol obstructs the enzyme emitter site. *Int. J. Biol. Macromol.* **117**, 617-624. (https://doi.org/10.1016/j.ijbiomac.2018.05.160)
61. Mallefet J, Duchatelet L, Coubris C. 2020 Bioluminescence induction in the ophiuroid *Amphiura filiformis* (Echinodermata). *J. Exp. Biol.* **223(4)**, jeb218719. (https://doi.org/10.1242/jeb.218719)

62. Mallefet J, Martinez-Soares P, Eléaume M, O'Hara T, Duchatelet L. 2023 New insights on crinoid (Echinodermata; Crinoidea) bioluminescence. *Front. Mar. Sci.* **10**, 1136138. (https://doi.org/10.3389/fmars.2023.1136138)
63. Loening AM, Fenn TD, Wu AM, Gambhir SS. 2006 Consensus guided mutagenesis of *Renilla* luciferase yields enhanced stability and light output. *Protein Eng. Des. Sel.* **19(9)**, 391–400. (https://doi.org/10.1093/protein/gzl023)
64. Tsuji FI, Ohmiya Y, Fagan TF, Toh H, Inouye S. 1995 Molecular evolution of the Ca^{2+}-binding photoproteins of the hydrozoa. *Photochem. Photobiol.* **62(4)**, 657-661. (https://doi.org/10.1111/j.1751-1097.1995.tb08713.x)
65. Powers ML, McDermott AG, Shaner NC, Haddock SHD. 2013 Expression and characterization of the calcium-activated photoprotein from the ctenophore *Bathocyroe fosteri*: Insights into light-sensitive photoproteins. *Biochem. Biophys. Res. Commun.* **431(2)**, 360-366. (https://doi.org/10.1016/j.bbrc.2012.12.026)
66. Burakova LP, Stepanyuk GA, Eremeeva EV, Vysotski ES. 2016 Role of certain amino acid residues of the coelenterazine-binding cavity in bioluminescence of light-sensitive Ca^{2+}-regulated photoprotein berovin. *Photochem. Photobiol. Sci.* **15**, 691-704. (https://doi.org/10.1039/c6pp00050a)
67. Burakova LP, Vysotski ES. 2019 Recombinant Ca2+-regulated photoproteins of ctenophores: Current knowledge and application prospects. *Appl. Microbiol. Biotechnol.* **103**, 5929-5946. (https://doi.org/10.1007/s00253-019-09939-0)
68. Jumper J, Evans R, Pritzel A, Green T, Figurnov M, Ronneberger O, *et al*. 2021 Highly accurate protein structure prediction with AlphaFold. *Nature* **596**, 583-589. (https://doi.org/10.1038/s41586-021-03819-2)
69. Abramson J, Adler J, Dunger J, Evans R, Green T, Pritzel A, *et al.* 2024 Accurate structure prediction of biomolecular interactions with AlphaFold 3. *Nature* **630**, 493-500. (https://doi.org/10.1038/s41586-024-07487-w)
70. Stepanyuk GA, Liu Z-J, Markova SS, Frank LA, Lee J, Vysotski ES, Wang B-C. 2008 Crystal structure of coelenterazine-binding protein from *Renilla muelleri* at 1.7Å: Why it is not a calcium-regulated photoprotein. *Photochem. Photobiol. Sci.* **7**, 442-447. (https://doi.org/10.1039/b716535h)
71. Buskey EJ, Stearns DE. 1991 The effects of starvation on bioluminescence potential and egg release of the copepod *Metridia longa*. *J. Plankton Res.* **13(4)**, 885-893. (https://doi.org/10.1093/plankt/13.4.885)
72. Thomson CM, Herring PJ, Campbell AK. 1995 Evidence for *de novo* biosynthesis of coelenterazine in the bioluminescent midwater shrimp, *Systellaspis debilis* C. *J. Mar. Biol. Assoc. U.K.* **75(1)**, 165-171. (https://doi.org/10.1017/S0025315400015277)
73. Oba Y, Kato S-I, Ojika M, Inouye S. 2009 Biosynthesis of coelenterazine in the deep-sea copepod, *Metridia pacifica*. *Biochem. Biophys. Res. Commun.* **390(3)**, 684-688. (https://doi.org/10.1016/j.bbrc.2009.10.028)

74. Bessho-Uehara M, Huang W, Patry WL, Browne WE, Weng J-K, Haddock SHD. 2020 Evidence for *de novo* biosynthesis of the luminous substrate coelenterazine in ctenophores. *iScience* **23(12)**, 101859. (https://doi.org/10.1016/j.isci.2020.101859)
75. Francis WR, Shaner NC, Christianson LM, Powers ML, Haddock SHD. 2015 Occurrence of isopenicillin-N-synthase homologs in bioluminescent ctenophores and implications for coelenterazine biosynthesis. *PLoS ONE* **10(6)**, e0128742. (https://doi.org/10.1371/journal.pone.0128742)
76. Haddock SHD, Rivers TJ, Robison BH. 2001 Can coelenterates make coelenterazine? Dietary requirement for luciferin in cnidarian bioluminescence. *Proc. Ntl Acad. Sci.* **98(20)**, 11148-11151.(https://doi.org/10.1073/pnas.201329798)
77. Herring PJ. 1991 Observations on bioluminescence in some deep-water anthozoans. In *Coelenterate Biology: Recent Research on Cnidaria and Ctenophora, Proceedings of the Fifth International Conference on Coelenterate Biology*, Southampton, UK, 10–14 July 1989; Springer: Dordrecht, The Netherlands; pp. 573–579.
78. Coubris C, Duchatelet L, Delroisse J, Bayaert WS, Parise L, Eloy MC, Pels C, Mallefet J. 2024 Maintain the light, long-term seasonal monitoring of luminous capabilities in the brittle star *Amphiura filiformis*. *Sci. Rep. Submitted.*
79. Herring P.J. 1978 Bioluminescence of invertebrates other than insects. In: Herring P.J. (ed), *Bioluminescence in action*, New York Academic Press, pp.199-240.
80. Inouye S, Watanabe K, Nakamura H, Shimomura O. 2000 Secretional luciferase of the luminous shrimp *Oplophorus gracilirostris*: cDNA cloning of a novel imidazopyrazinone luciferase. *FEBS Lett.* **481(1)**, 19-25. (https://doi.org/10.1016/S0014-5793(00)01963-3)
81. Kobilka B. 1992 Adrenergic receptors as models for G protein-coupled receptors. *Ann. Rev. Neurosci.* **15(1)**, 87-114. (https://doi.org/10.1146/annurev.ne.15.030192.000511)
82. Caron MG, Lefkowitz RJ. 1993 Catecholamine receptors: structure, function, and regulation. *Recent Prog. Horm. Res.* **1993**, 277-290. (https://doi.org/10.1016/B978-0-12-571148-7.50014-2)
83. Neves SR, Ram PT, Iyengar R. 2002 G protein pathways. *Science* **296(5573)**, 1636-1639. (https://doi.org/10.1126/science.1071550)
84. Brown AM, Birnbaumer L. 1988 Direct G protein gating of ion channels. *Am. J. Physiol. Heart Circ. Physiol.* **254(3)**, H401-H410. (https://doi.org/10.1152/ajpheart.1988.254.3.H401)
85. Hille B. 1994 Modulation of ion-channel function by G-protein-coupled receptors. *Trends Neurosci.* **17(12)**, 531-536. (https://doi.org/10.1016/0166-2236(94)90157-0)
86. Dolphin AC. 2003 G protein modulation of voltage-gated calcium channels. *Pharmacol. Rev.* **55(4)**, 607-627. (https://doi.org/10.1124/pr.55.4.3)
87. Tedford HW, Zamponi GW. 2006 Direct G protein modulation of Cav2 calcium channels. *Pharmacol. Rev.* **58(4)**, 837-862. (https://doi.org/10.1124/pr.58.4.11)
88. Roda A, Pasini P, Mirasoli M, Michelini E, Guardigli M. 2004 Biotechnological applications of bioluminescence and chemiluminescence. *Trends Biotechnol.* **22(6)**, 295-303. (https://doi.org/10.1016/j.tibtech.2004.03.011)

89. Kirkpatrick A, Xu T, Ripp S, Sayler G, Close D. 2019 Biotechnological advances in luciferase enzymes. *Bioluminescence-Analytical Applications and Basic Biology*, 1-23. (https://doi.org/10.5772/intechopen.85313)
90. Welsh DK, Kay SA. 2005 Bioluminescence imaging in living organisms. *Curr. Opin. Biotechnol.* **16(1)**, 73-78. (https://doi.org/10.1016/j.copbio.2004.12.006)

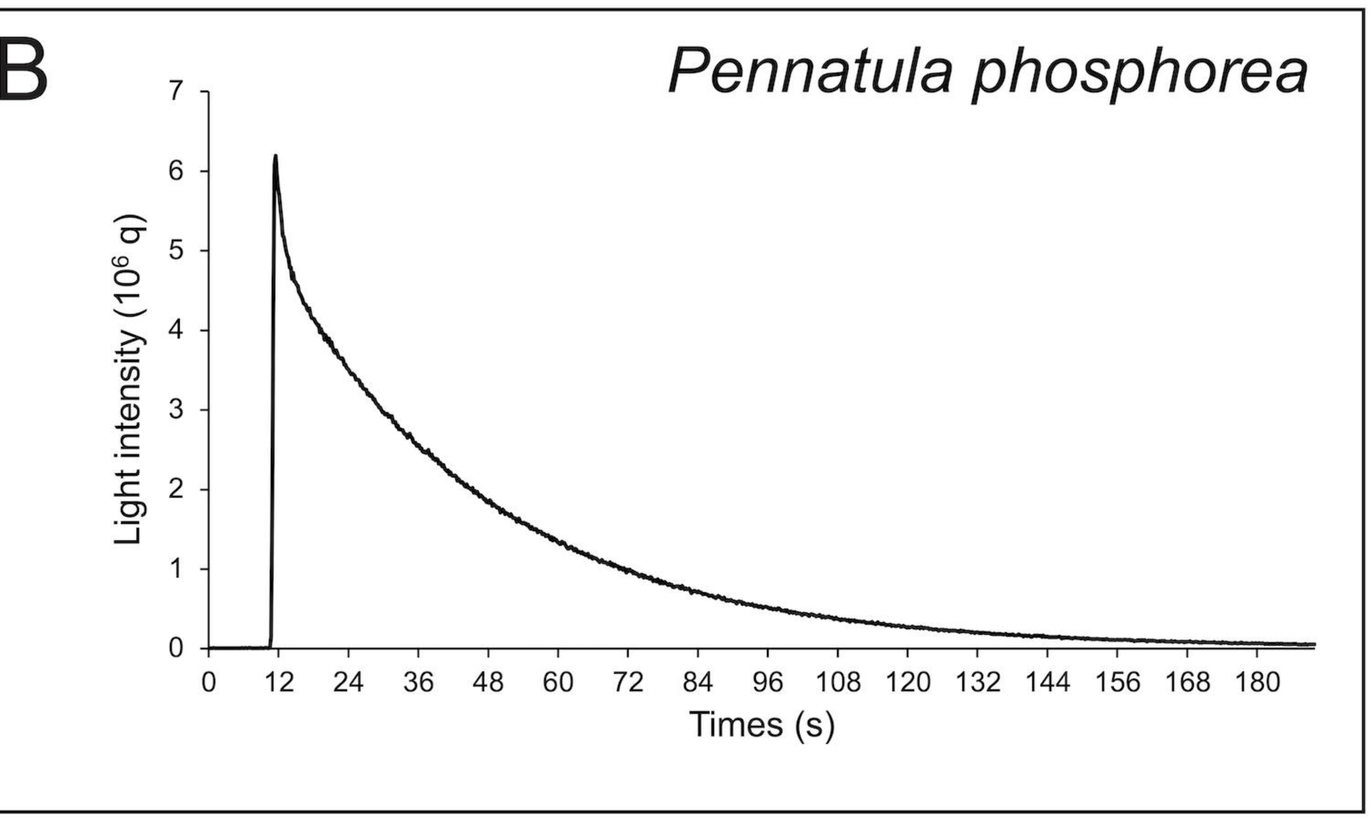

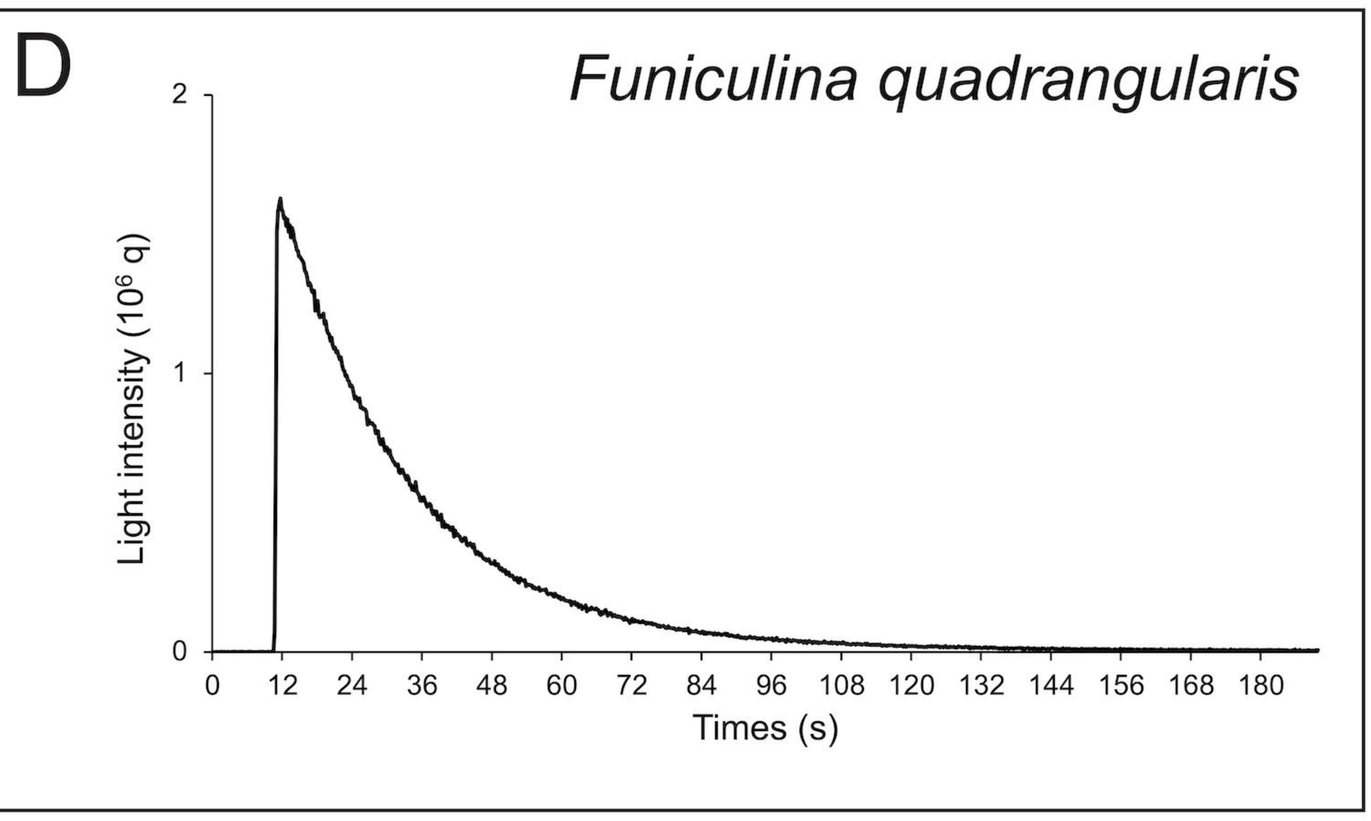

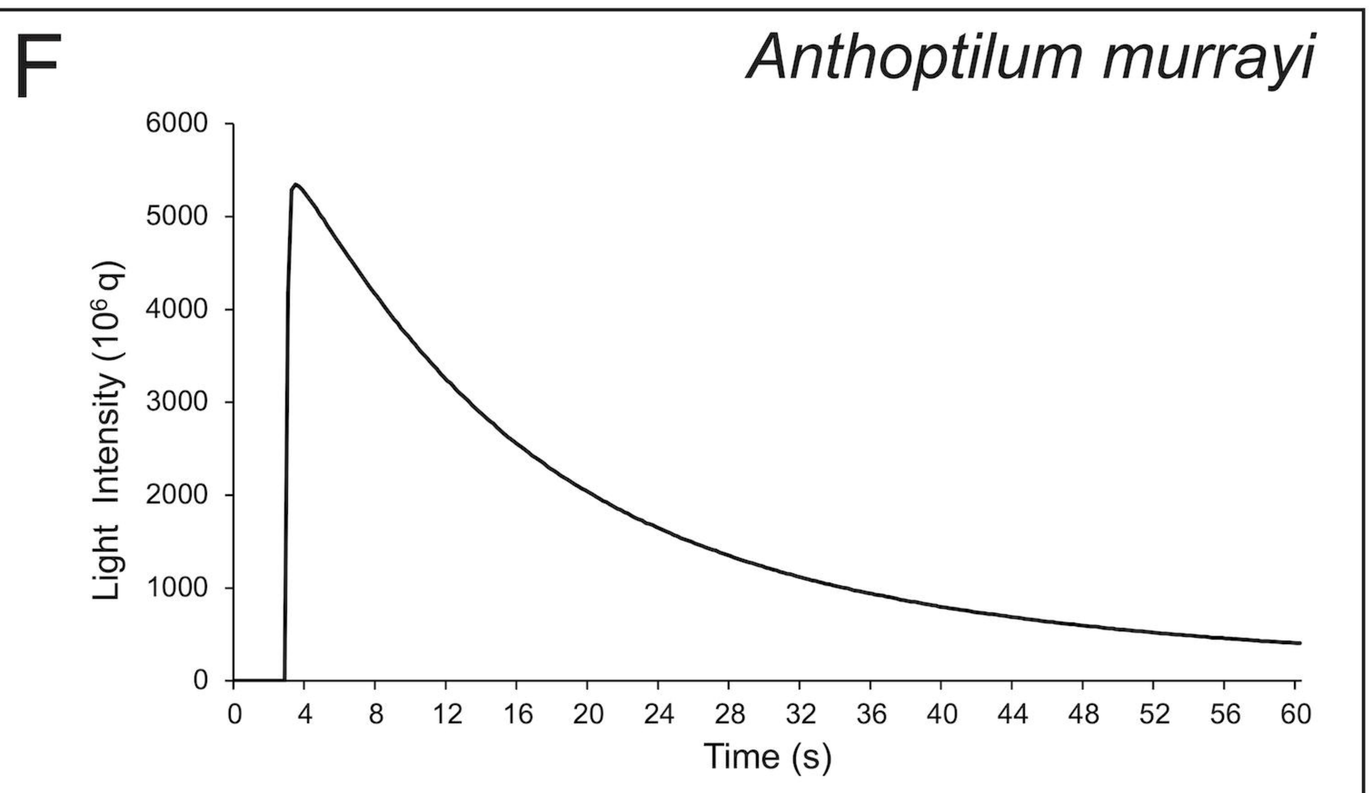

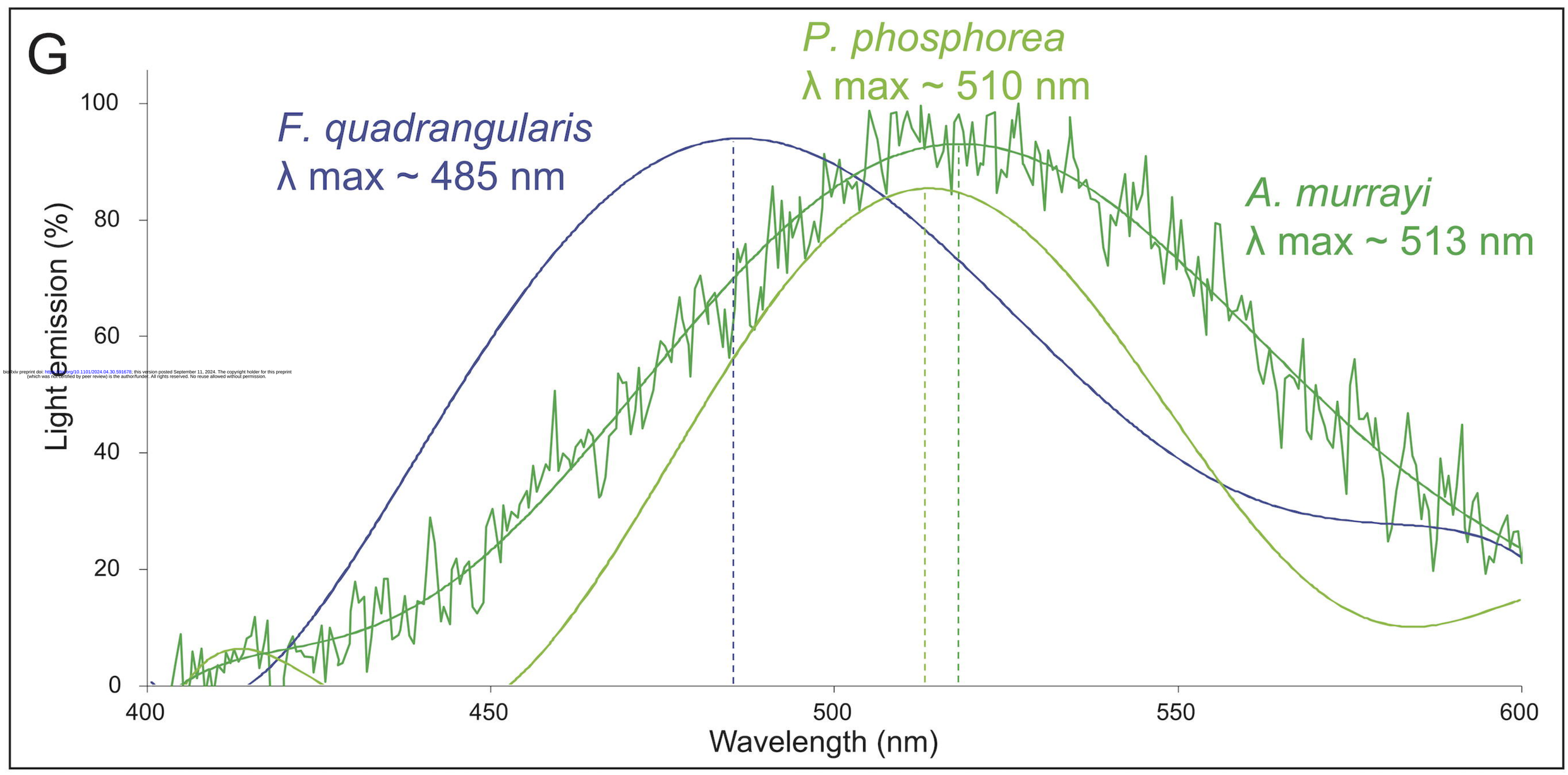

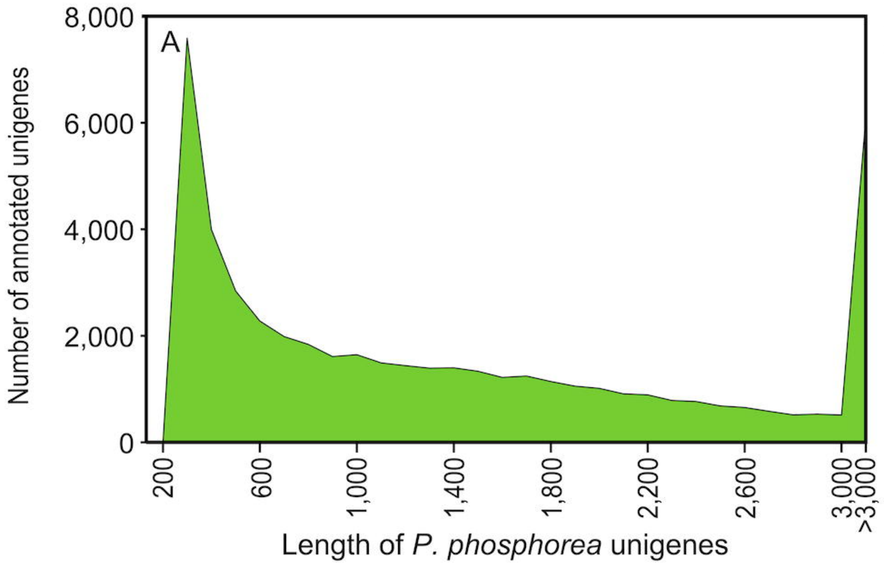

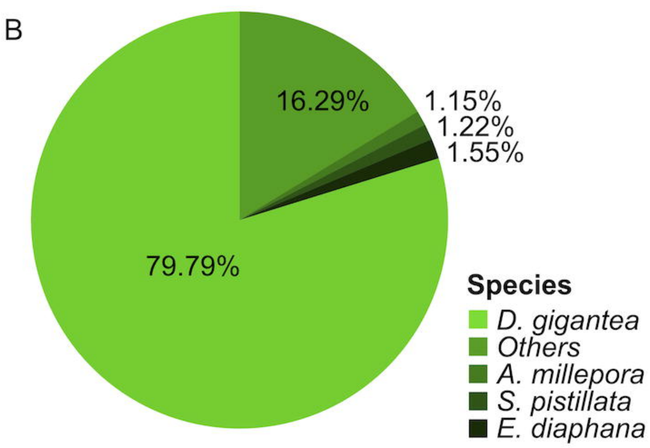

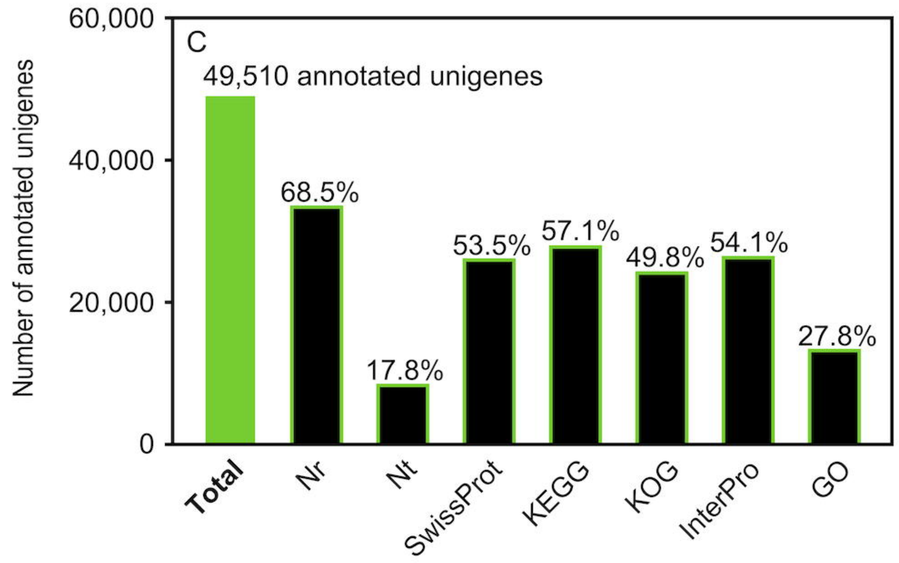

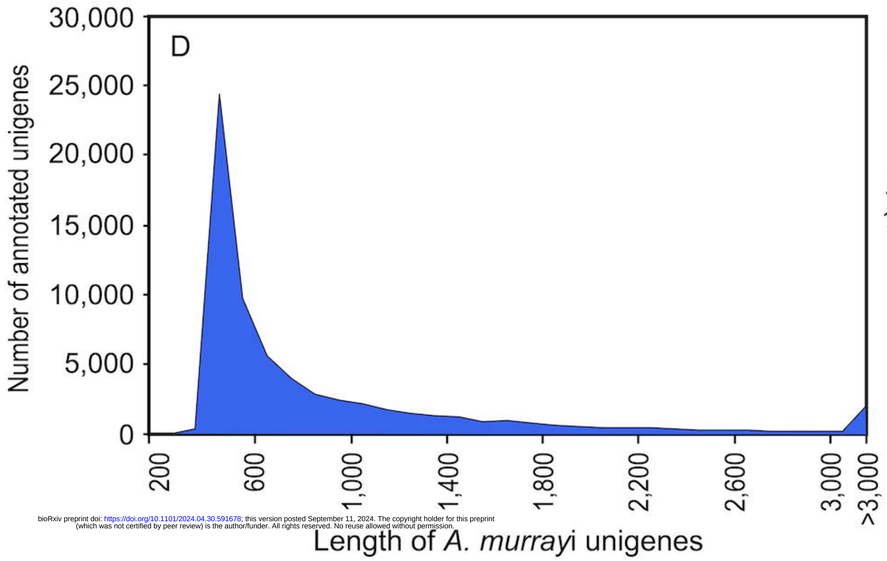

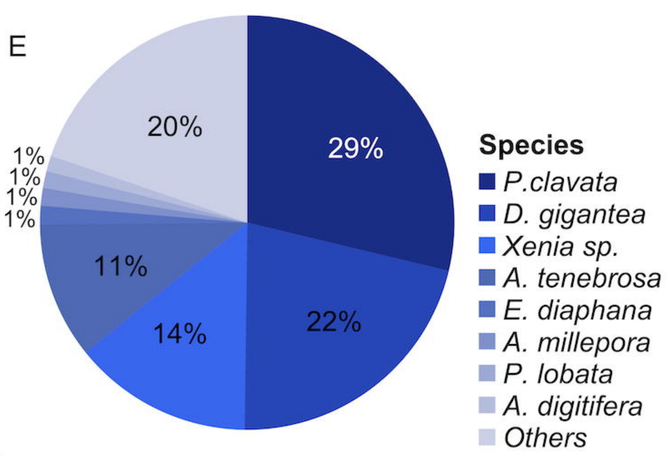

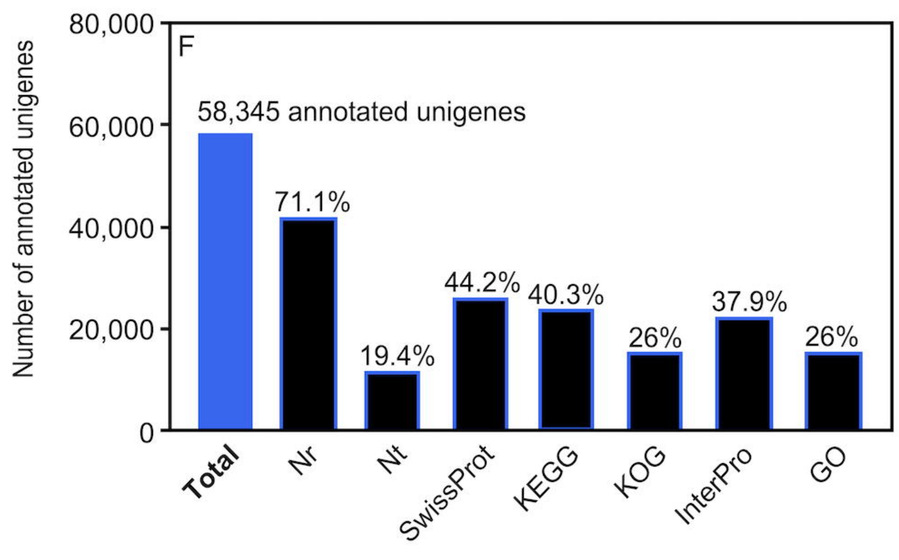

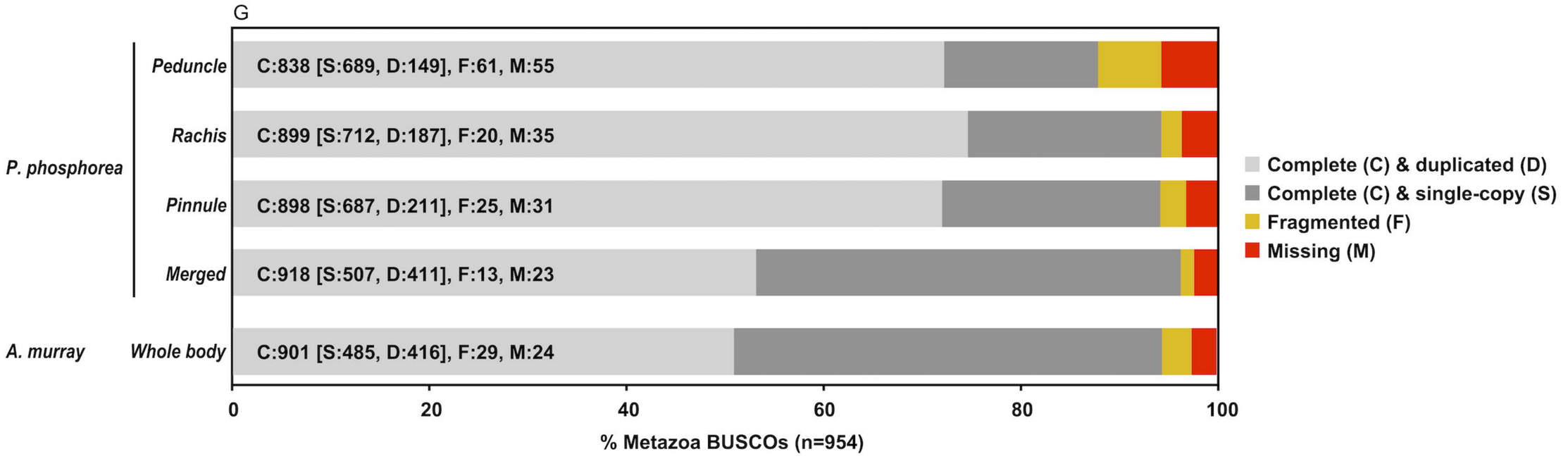

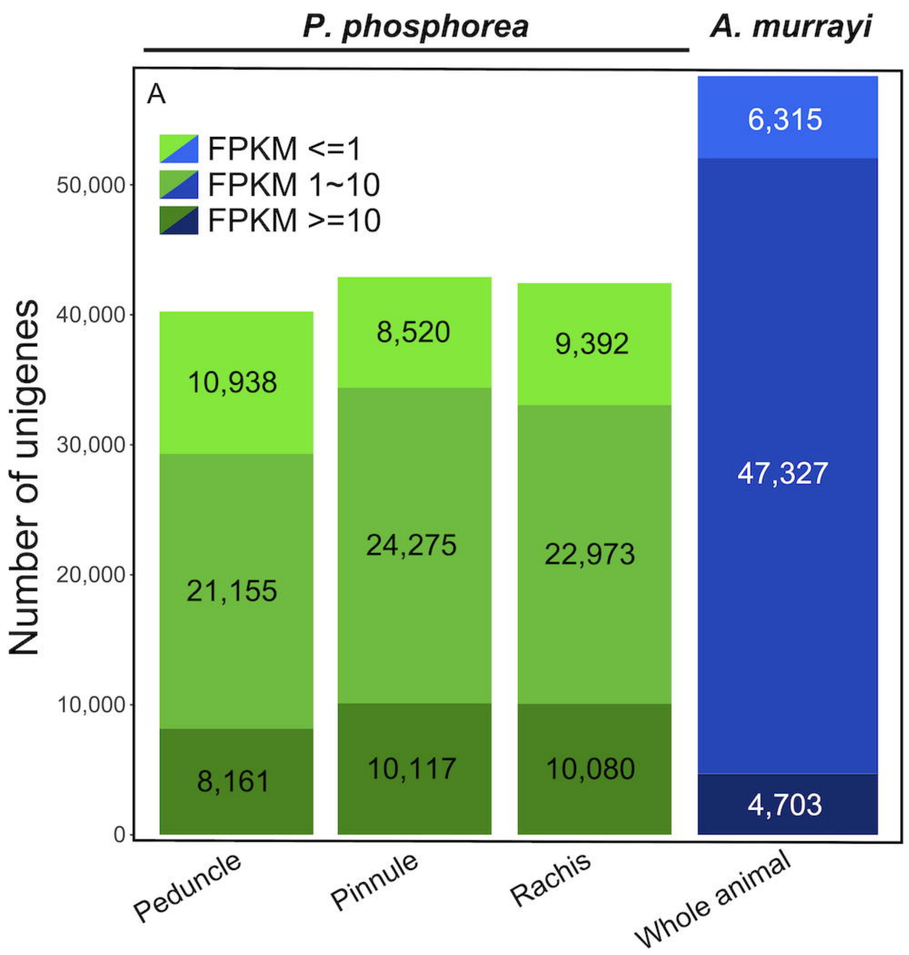

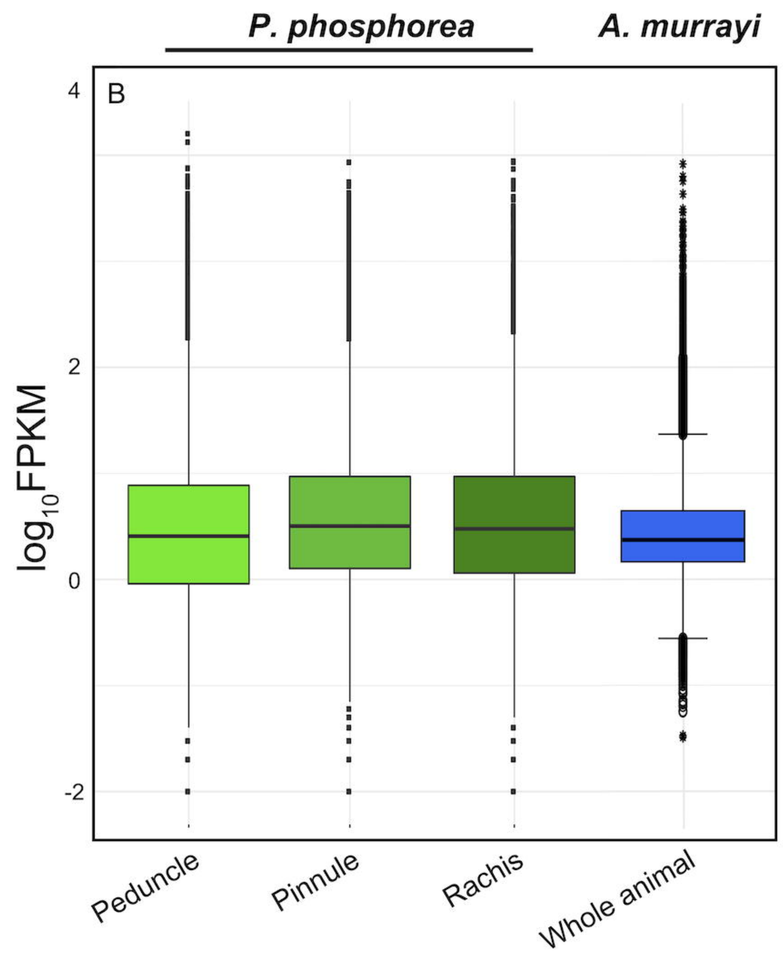

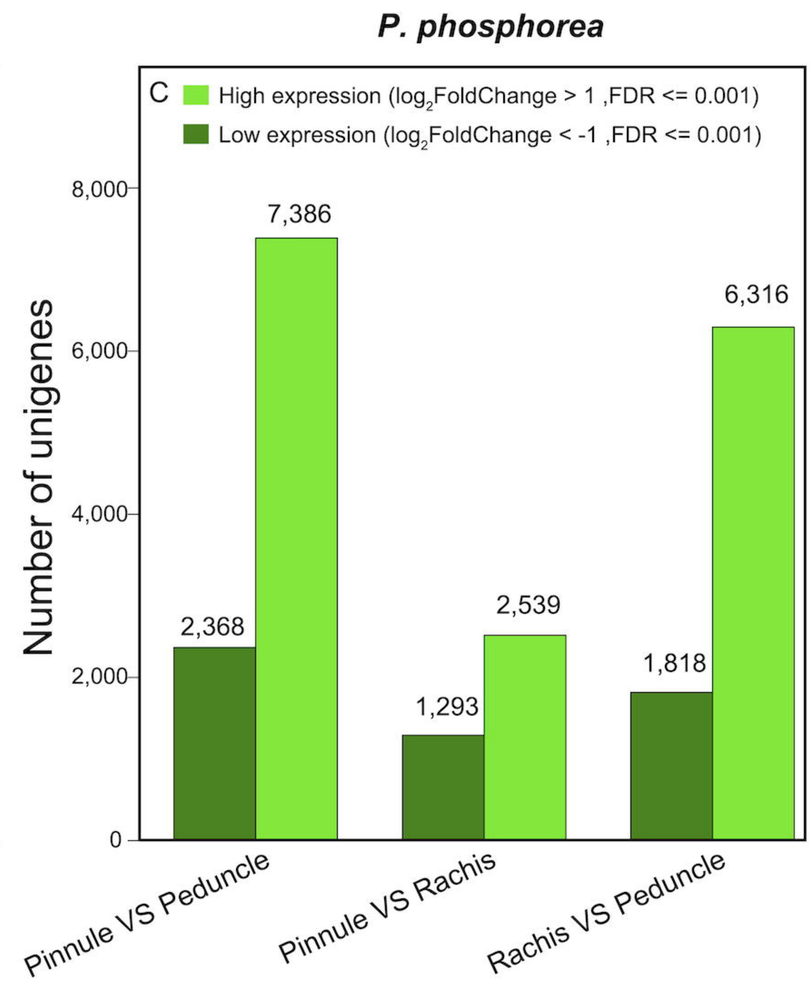

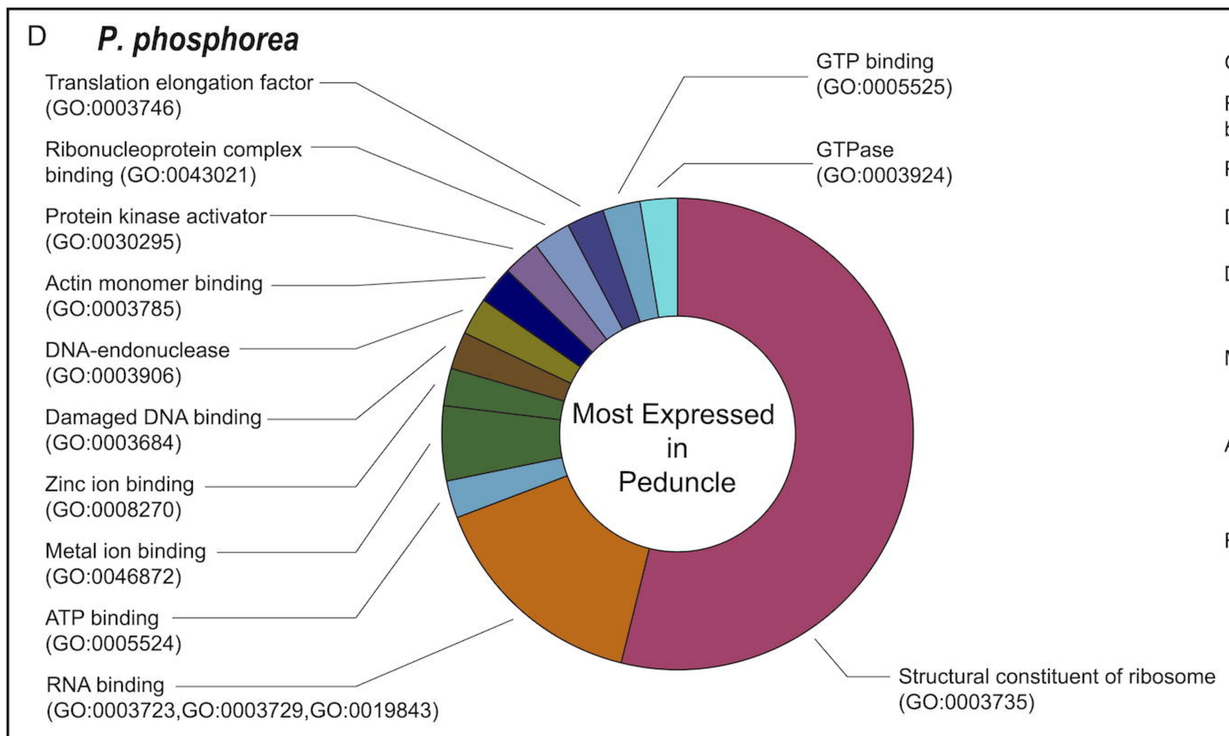

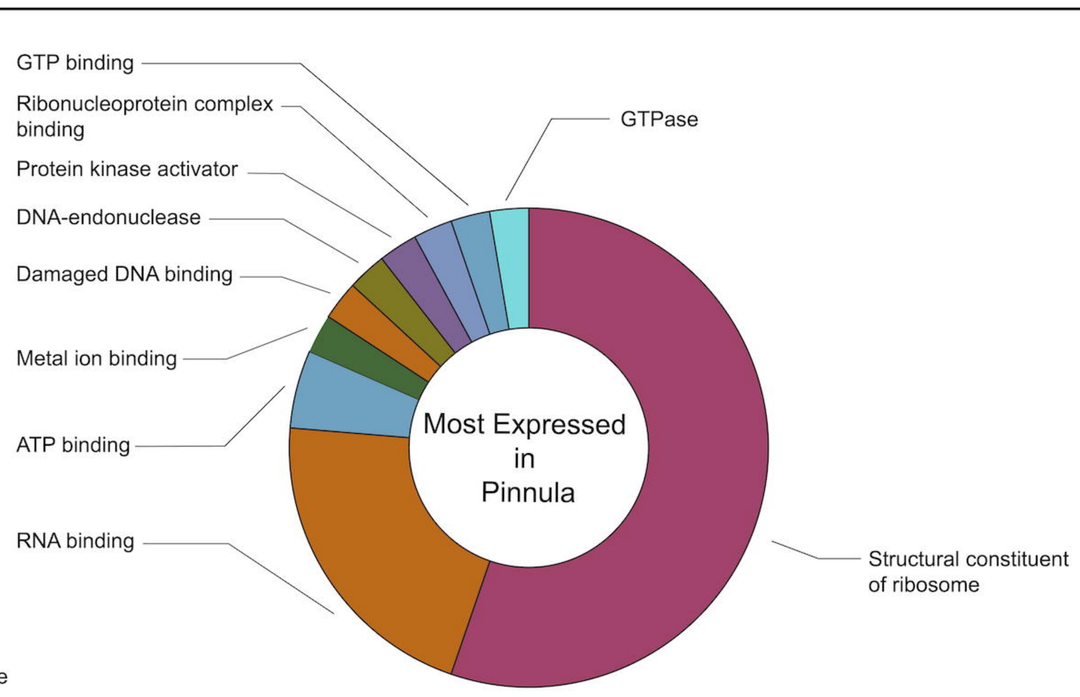

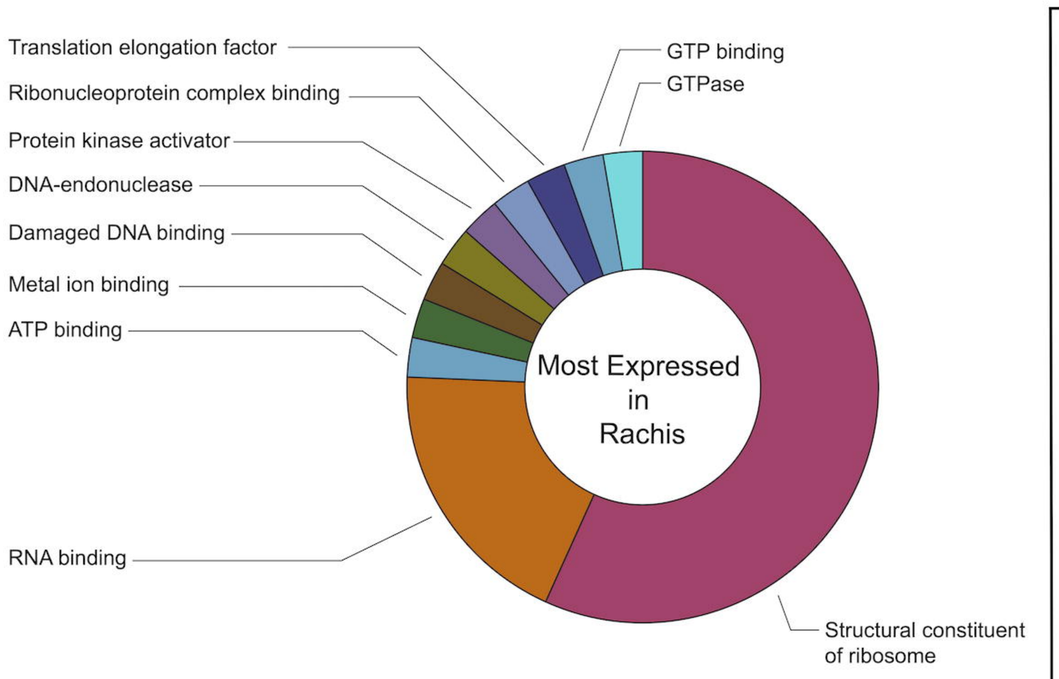

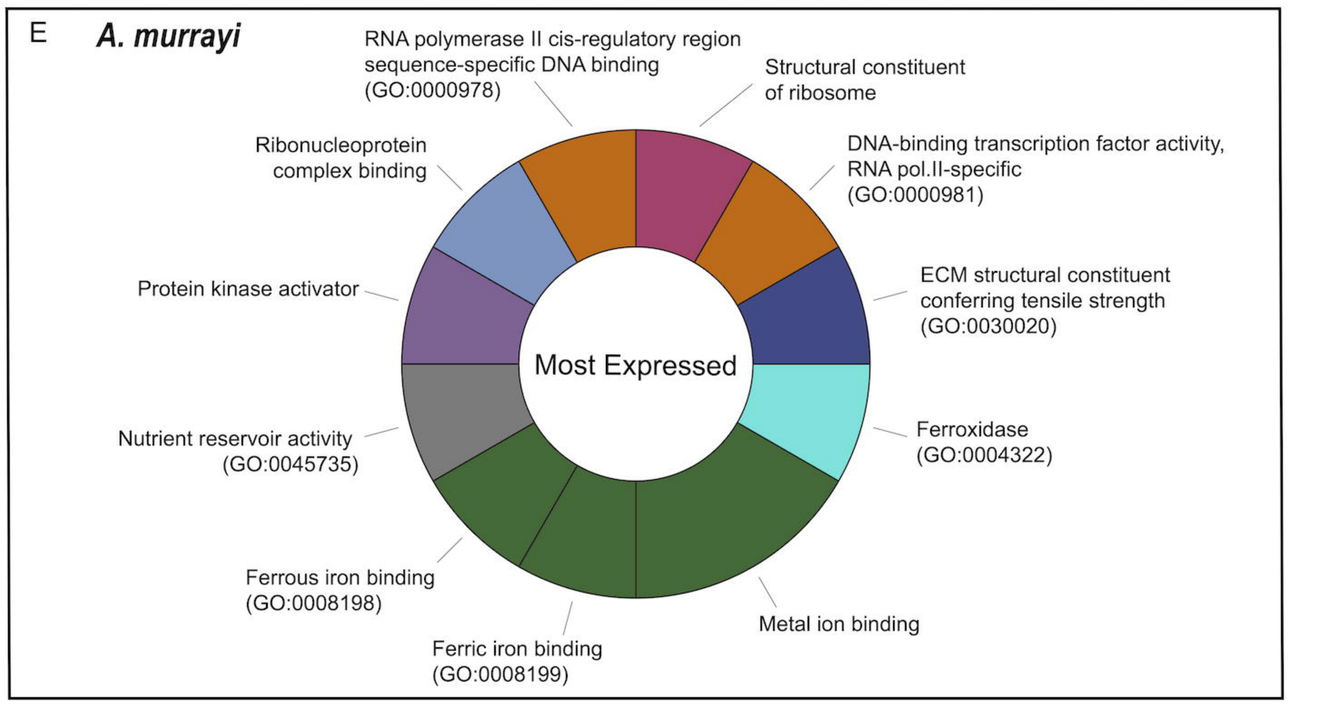

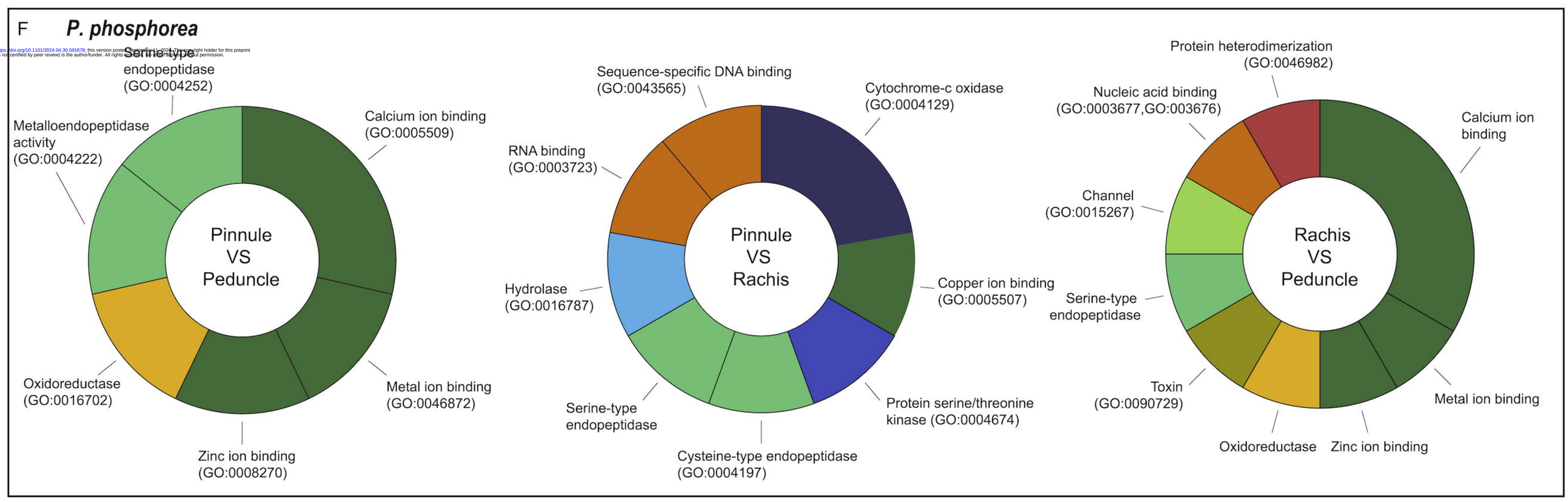

A

RLuc enzyme Clade A

RLuc-like enzyme Clade B

RLuc-like enzyme Clade C

0.3

100 A. murrayi
100
C. obesa
100
89 P. phosphorea
100
R. reniformis
85 R. muelleri

100 A. murray
90
100 R. reniformis
R. muelleri
98 P. phosphorea
Xenia sp
P. flava a
P. flava b
P. clavata
T. musica
S. cruciata
98 D. gigantea

89 A. murrayi
R. muelleri
99 P. phosphorea

85 S. cruciata
82 T. musica
P. flava
98 D. gigantea

100 S. purpuratus
43 S. kovalevskii
B. floridae
C. intestinalis

100 Outgroup
(Bacterial haloalkane dehalogenases)

86
100
78
97
89
78
97
100

Deuterostome
RLuc-like enzymes

P. phosphorea
A. murrayi
Pinnula
Rachis
Peduncle
Whole

B
C

comp24811
CL1333.contig1
CL1333.contig2
comp24802
Unigene12757
comp31557
CL1771.contig1
CL1771.contig2
CL1771.contig3
CL1771.contig4

Log_{10}(FPKM+1): 0.02 1.38 / 0.41 2.39

Malacalcyonacea, Octocorallia
Scleralcyonacea, Octocorallia
Deuterostoma
Bacteria

D

R. reniformis LUC (RLUC)
PDB ID: 7OMR

P. phosphorea LUC
AlphaFold model

A. murrayi LUC
AlphaFold model

CEI
N
C

All superposed

Helical cap

αβα-sandwich core

E

λmax ~ 498 nm
λmax ~ 513 nm
Light emission (%)
Wavelength (nm)
0 20 40 60 80 100 120
400 461 523 585

Tuning emission wavelength
V185
M185
M179
D162
D162
D156
N53
N53
N47
CEI
Dioxygen binding
D120
D120
D114
H285
H285
H278
W121
W121
W115
E144
E144
E138
Proton-relay system

A

GFPs Octocorallia

100 A. murrayi
99 99 A. murrayi
96 C. obesa
100 R. reniformis GFP
82 P. phosphorea
100 Ptilosarcus sp.
99 P. gurneyi
94 R. muelleri
56 R. reniformis
85 D. gigantea
58 P. clavata
94 Xenia sp.
S. gracillimum
Dendronephthya sp.
Clavularia sp.
Sarcophyton sp.

0.3

GFPs Hexacorallia

100 Scleractinia
Scleractinia/Corallimorpharia
100 Scleractinia
91 Scleractinia/Actiniaria/Zoantharia
Actiniaria
100 Ceriantharia
100 Outgroup (Hydrozoa GFPs)

P. phosphorea

B

Pinnule Rachis Peduncle

CL380.contig2
CL380.contig4
CL380.contig5
CL380.contig6
CL380.contig7
CL380.contig8
CL380.contig9
CL380.contig10
CL380.contig12
Unigene11330
Unigene11331
Unigene16546

Log_{10}(FPKM+1): 0 1.90

A. murrayi

C

Whole

comp33799
comp24361

Log_{10}(FPKM+1):
0.24 1.02

Malacalcyonacea, Octocorallia
Scleralcyonacea, Octocorallia
Hexacorallia
Hydrozoa

D

R. reniformis GFP (RGFP)
PDB ID: 2RH7

N C C N CRO

P. phosphorea GFP
AlphaFold model

P. phosphorea specific loop extension

A. murrayi GFP
AlphaFold model

All superposed

A

Coelenterazine binding-proteins

Renilla sp CBPs
***P. phosphorea* CBPs**
***A. murrayi* CBPs**
Renilla sp CBP-like
***P. phosphorea* CBP-like**
***A. murrayi* CBP-like**
***A. murrayi* CBP-like**
***A. murrayi* CBP-like**
P. clavata CBP-like
D. gigantea CBP-like

Photoprotein-like

Renilla sp
P. phosphorea
A. murrayi
P. phosphorea
PPb-like
A. murrayi
P. phosphorea
Ctenophora
N. vectensis
P. clavata (1)
D. gigantea
P. clavata (2,3)
PPa-like
Renilla sp
P. phosphorea
A. murrayi
Hydrozoa
Porifera

0.3

SARC

Outgroup (Calmodulins)

B

P. phosphorea

Pinnula
Rachis
Peduncle

CL1544.contig1
CL1544.contig2
Unigene12032
Unigene10436
CL2172.contig1
CL2172.contig2
CL2172.contig3
Unigene10367
Unigene502
Unigene4438

Log_{10}(FPKM+1): 0 2.85

C

A. murrayi

Whole

Comp21366
Comp32611
Comp22336
Comp99008
Comp6286
Comp27071
Comp23804
Comp8021
Comp23501
Comp21144

Log_{10}(FPKM+1): 0.18 2.38

Malacalcyonacea, Octocorallia
Scleralcyonacea, Octocorallia
Hexacorallia
Hydrozoa
Porifera
Ctenophora

D

R. muelleri CBP (RCBP)
PDB ID: 2HPS

P. phosphorea CBP
AlphaFold model

A. murrayi CBP
AlphaFold model

All superposed

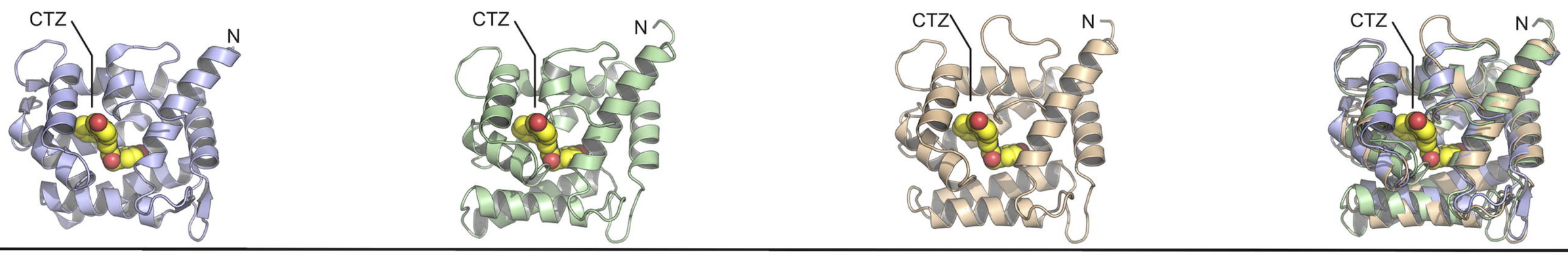

Pennatula phosphorea

A

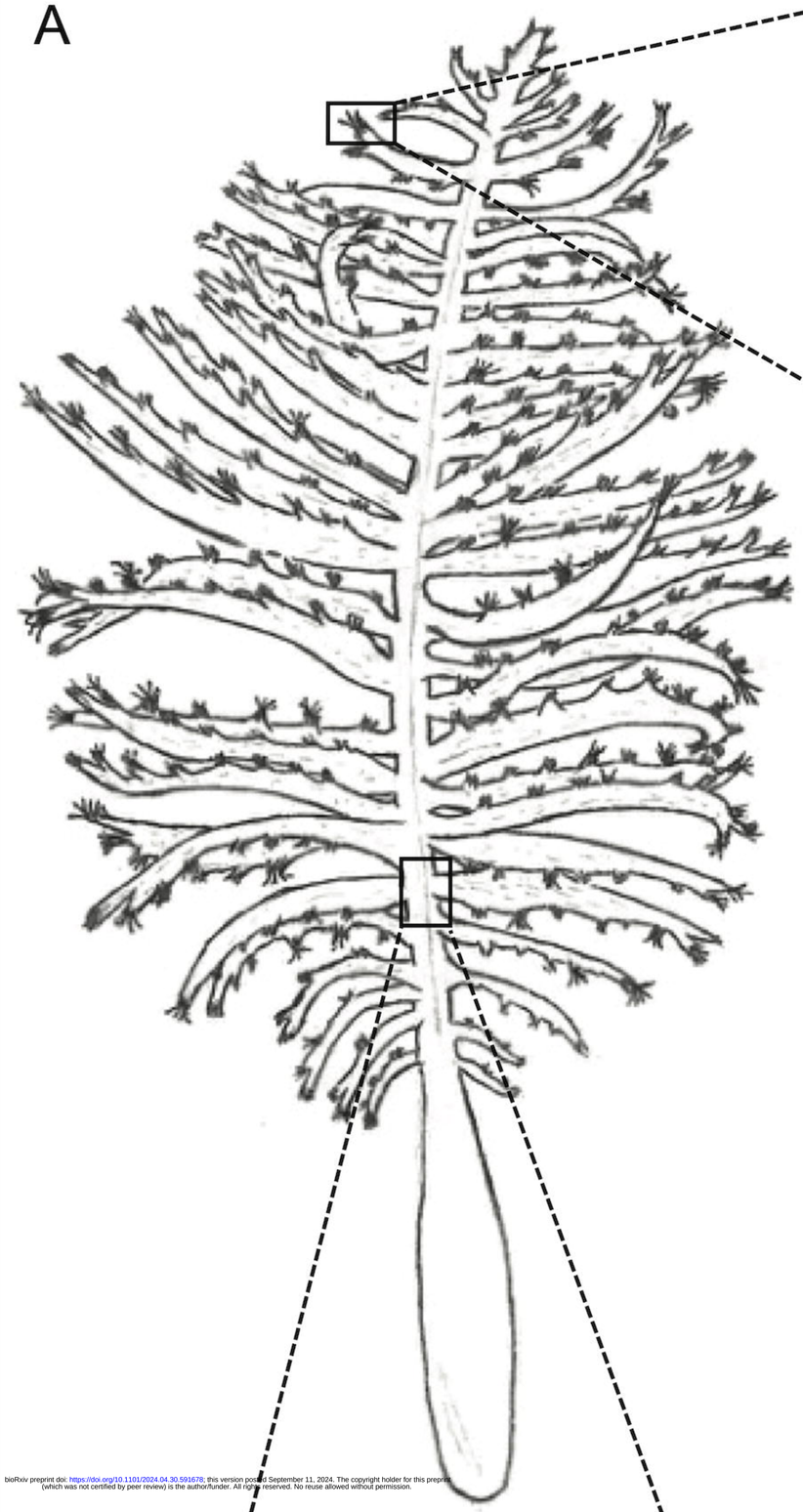

B

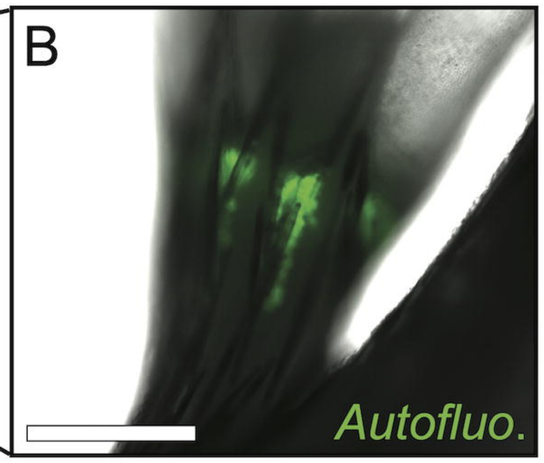

C

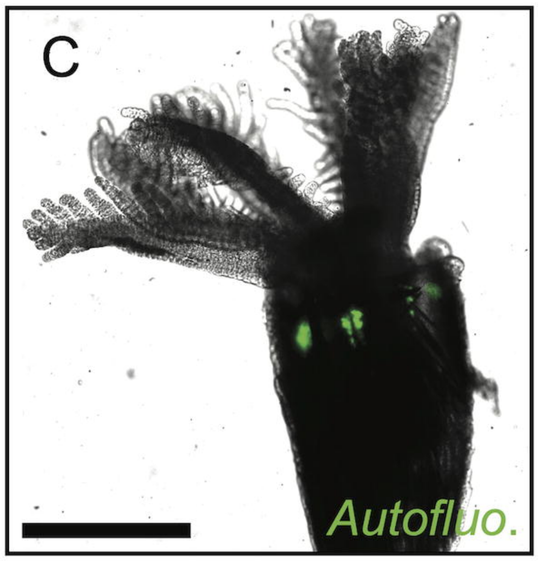

D

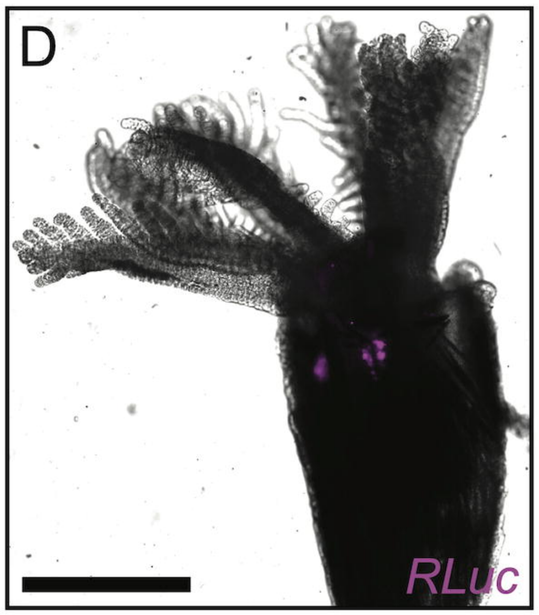

E

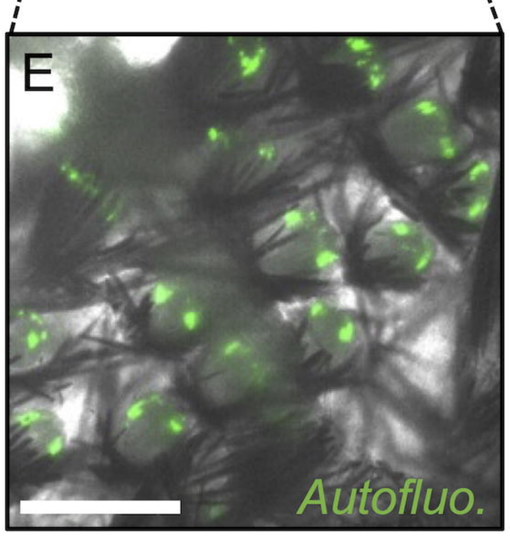

F

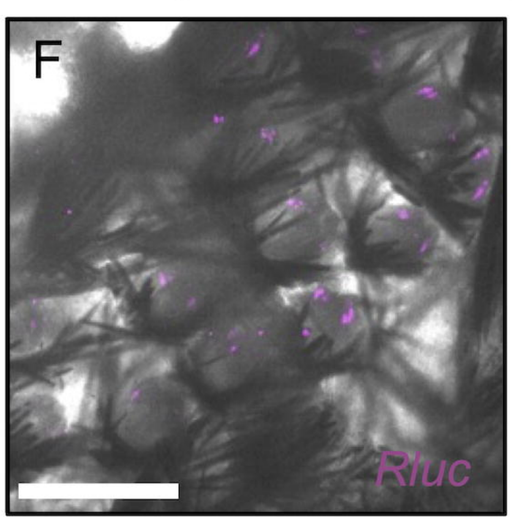

Funiculina quadrangularis

G

H

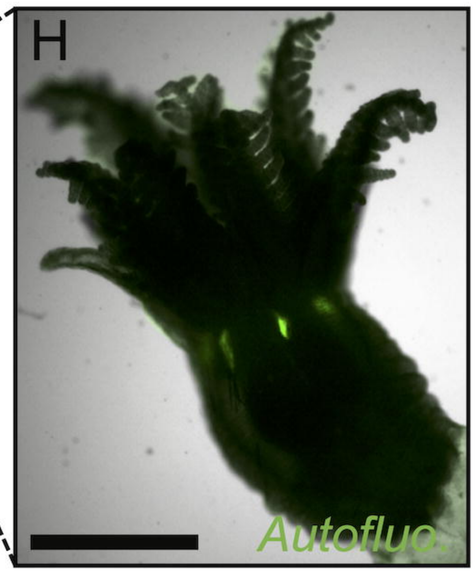

I

J

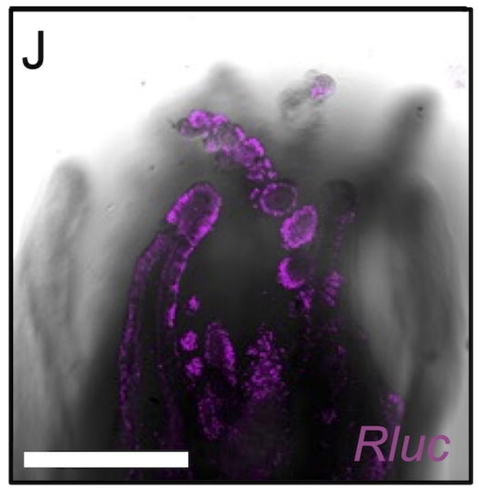

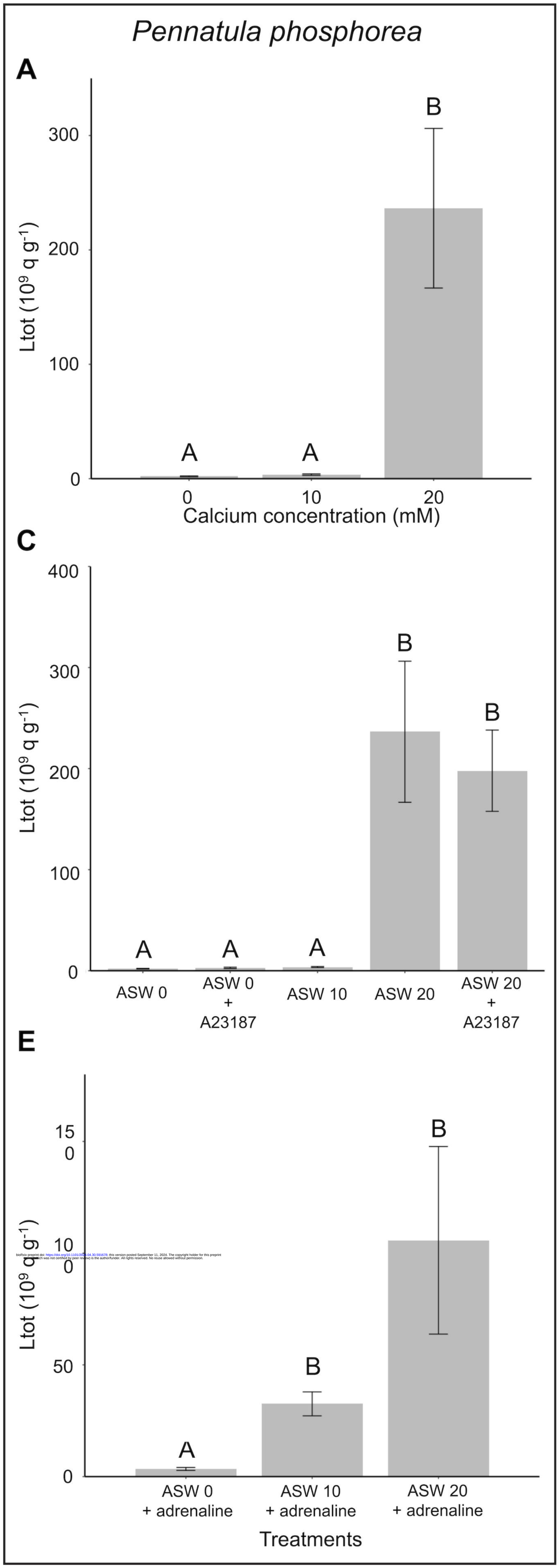

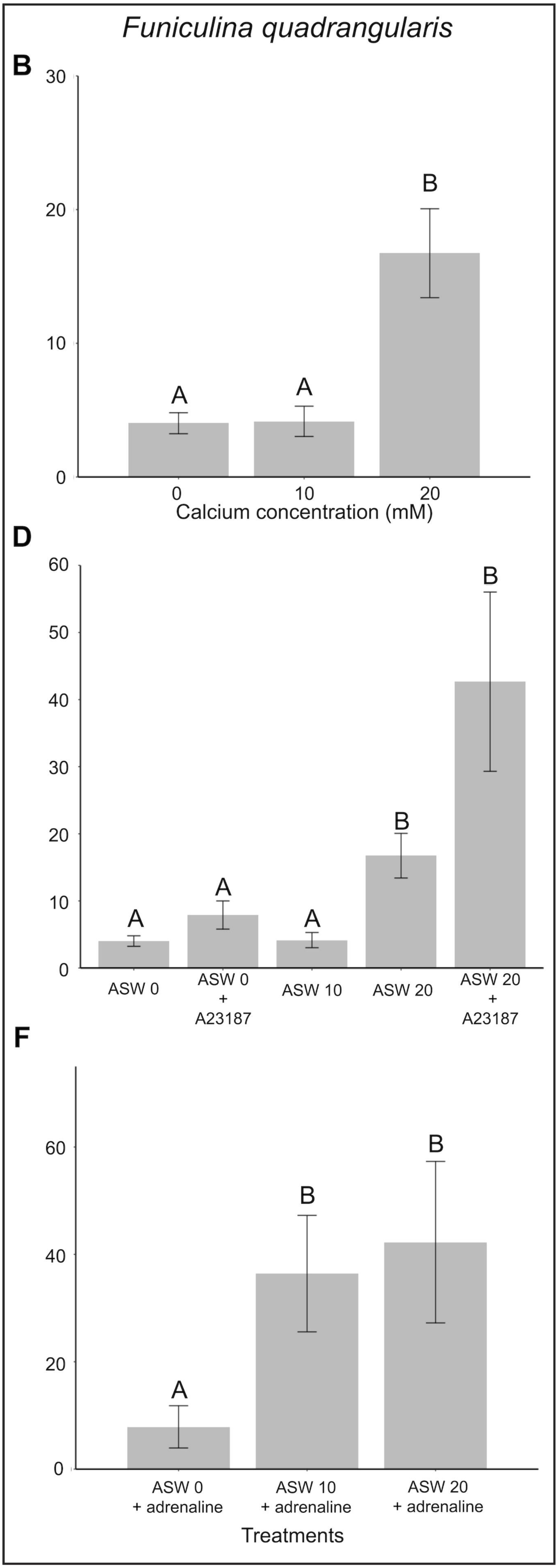

Extracellular

Intracellular

Pennatula phosphorea
Anthoptilum murrayi

Funiculina quadrangularis

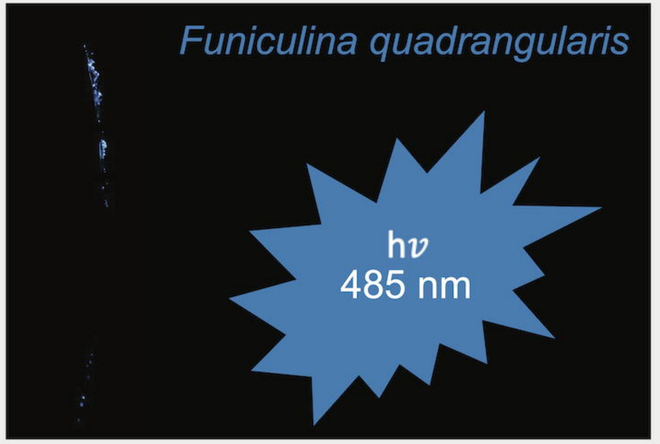

Catecholamine

G

+

Ca^{2+}

CTZ

CBP

LUC

O_2

CTM + CO_2 +

GFP

hν
480 nm